Title
Enhanced Inhibitory Neurotransmission as a Therapeutic Target in ApoE4-Related Alzheimer's Disease

Author
Nova, Philip W.

Publication Date
2017

Peer reviewed|Thesis/dissertation

Enhanced Inhibitory Neurotransmission as a Therapeutic Target in ApoE4-Related Alzheimer's Disease

by

Philip Nova

DISSERTATION

Submitted in partial satisfaction of the requirements for the degree of

DOCTOR OF PHILOSOPHY

in

Biomedical Sciences

in the

GRADUATE DIVISION

of the

UNIVERSITY OF CALIFORNIA, SAN FRANCISCO

DEDICATION

This work is dedicated to my grandpa Bill Hoover, MD and PhD, who inspired me to become a scientist and suffered from Alzheimer's disease;

to my grandma, Arlene Hoover: thanks for always being proud of me. I hoped you'd be at my graduation but I didn't quite finish in time;

and to all the shoulders I've leaned on over the past 5 years, especially Hane, Mom, Dad, and Jenny; I couldn't have done it without you.

ACKNOWLEDGEMENTS

This work would not have been possible without the support of my research mentor Yadong Huang and my thesis committee members Jeanne Paz and Sheng Ding. Yadong Huang was an invaluable source of encouragement and expertise throughout the process of completing this work, and always inspired with his optimism and deep knowledge. Jeanne Paz graciously welcomed me to her lab meetings, provided hands-on training in slice physiology, and established a fruitful collaboration between my lab and hers. Sheng Ding provided insightful guidance and much-needed expertise in pharmacology to the project.

I am grateful to the many members of the Huang lab and other GIND labs who have provided their time and energy, particularly with regard to training me in new techniques. I have learned greatly from current and former lab members including David Walker, Maureen "Reeny" Balestra, Qin Xu, Mary Jeong, Anna Gillespie, Leslie Tong, Johanna Knoeferle, Laura Leung, Chengzhong Wang, Victoria Yoon, Jessie Carr, Alice Taubes, Emily Jones, Ramsey Najm, Hung Lin, and Misha Zilberter. To mention a few whose contributions to my education go beyond the scope of this thesis: Reeny, for teaching me cell culture; Anna and Emily, for collaborating on *in vivo* electrophysiology; Stephanie Holden and Biljana Djukic, for collaborating on *in vitro* electrophysiology; and Leslie Tong, whose thesis provided much of the essential background for my own work. Many thanks to Theodora Pak for scheduling meetings, booking rooms, and saving me much time and many headaches. Thank you as well to David Walker for invaluable training in molecular biology and many thoughtful conversations; rest in peace.

This work was supported by the J. David Gladstone Institute, the National Institutes of Health, and the National Science Foundation.

CONTRIBUTIONS

Victoria (Seo Yeon) Yoon bred and maintained the apoE knock-in (apoE-KI) and Dlx-Cre/floxed knock-in mouse lines, assisted with behavior studies (e.g. rodent transfers, single housing for behavior), and performed the behavior studies for the bumetanide-treated mice. Victoria, Emily Jones, and Alice Taubes provided additional assistance with bumetanide injections.

Leslie Tong and Laura Leung provided protocols, training, and expertise for immunohistochemistry.

The lentiviral expression vector was provided as a generous gift from Takashi Miyamoto in the Lennart Mucke lab, and was originally developed by Michael Ward in the Li Gan lab. The open reading frame for δ was subcloned into the lentiviral expression vector by David Walker.

Ramsey Najm provided assistance on the Keynce microscope. Leslie Tong and Anna Gillespie provided training on stereotaxic injection of lentivirus. Mary Jeong and Qin Xu provided training for Western Blotting and generously shared antibodies and reagents. Training for the behavior assays was provided by Michael Gill and Iris Lo of the Gladstone Behavior Core.

Yadong Huang conceived of the original ideas for the studies presented here, conducted the essential background work on ApoE and Alzheimer's disease, and obtained the grant funding to support this research.

ABSTRACT

Enhanced Inhibitory Neurotransmission as a Therapeutic Target in ApoE4-Related Alzheimer's Disease

Philip Nova

ApoE4 is the main genetic risk factor for Alzheimer's disease (AD) and causes dysfunction and death in inhibitory interneurons in humans and AD mouse models. In apoE4 knock-in mice (apoE4-KI), a model of late-onset AD, replacing lost inhibitory interneurons with GABAergic progenitors restores inhibition and rescues learning and memory behavior. Postsynaptic inhibitory transmission depends on receptors for the inhibitory neurotransmitter gamma-aminobutyric acid (GABA) and on the equilibrium potential for chloride (E_{Cl}). To determine whether increasing postsynaptic inhibitory transmission – rather than replacing lost interneurons themselves – rescues learning and memory in apoE4-KI mice, we evaluated two strategies to increase postsynaptic inhibition. The diuretic drug bumetanide hyperpolarizes E_{Cl} by inhibiting the chloride importer NKCC1 in neurons. We show that aged apoE4-KI mice have increased expression of NKCC1 and that chronic treatment with bumetanide normalizes learning and memory behavior. We also show that increasing expression of $GABA_A$ receptor subunit δ in the hippocampus of aged apoE4-KI mice rescues cognitive flexibility and anxiety-like behavior, and ameliorates inhibitory interneuron losses. These results suggest that postsynaptic inhibition is an effective, druggable target for apoE4-related AD with potential disease-modifying effects.

TABLE OF CONTENTS

LIST OF TABLES

LIST OF FIGURES

CHAPTER 1

Introduction

Alzheimer's Disease

Alzheimer's Disease (AD) is the most common cause of dementia. AD is characterized by progressive loss of memory and cognitive function, changes to personality, and ultimately death. Currently over 35 million people are affected worldwide; assuming current rates of growth, this number will triple in the next 40 years (Barnes and Yaffe, 2011). There are currently no effective treatments to halt or delay progression of the disease.

Efforts to develop disease-modifying AD therapeutics have been stymied by the complex, multifactorial nature of the disease (Huang and Mucke, 2012). Since its initial description in 1906, a wide variety of disease mechanisms have been identified, including: loss of brain volume in multiple brain regions, especially the hippocampus (Gomez-Isla et al., , 1996; Ball et al., 1985); loss of neuronal synapses and spines (Palop et al., , 2006); seizures and sub-seizure alterations in network activity (Larner et al., 2010; Palop and Mucke, 2010; Verret and Palop et al., , 2012); impairments in mitochondrial function, glucose metabolism, and energy homeostasis (Lin and Beal, 2006); increased DNA damage and impaired DNA repair (Coppede and Migliore, 2009); and changes to protein expression and trafficking (Tang et al., 2012). However, the majority of AD research to date has focused on histopathological hallmarks: in particular, intracellular accumulation of Tau and extracellular accumulation of amyloid-β (Aβ) (Bloom 2014).

The amyloid hypothesis, or the idea that Aβ is the key driver of AD, has dominated the search for AD therapeutics (Hardy and Selkoe, 2002; Citron, 2010). Aβ is the pathological

cleavage product of amyloid precursor protein (APP), a protein with unknown physiological function. While compounds targeting various aspects of Aβ production, deposition, and clearance have shown promising results in animal models (Citron, 2010), they have yielded disappointing results in human clinical trials (Golde et al., 2011; Mangialasche et al., 2010). Clinical failures for drugs targeting Aβ have been blamed on difficulties in determining the most effective time point for treatment (Golde et al., 2011); in addition, plaque deposition correlates poorly with disease progression (Giannakopoulos P et al., 2003) and the compensatory/homeostatic (Jedlickaa et al., 2012; Haass et al., 1992) versus causative role of Aβ in AD is still contested (Krstic and Knuesel, 2013).

Some difficulties in translating Aβ-targeting therapeutics into the clinic may also result from heterogeneity of disease mechanisms within the patient population. Initial support for the amyloid hypothesis came from genetic studies of families in which AD is transmitted in a Mendelian pattern; in these families, multiple mutations in either APP itself, or the APP processing pathway, were linked to familial AD (FAD) (Blennow et al., 2006). FAD is a particularly severe form of AD, is transmitted in an autosomal-dominant pattern, and leads to cognitive deficits before age 65. However, FAD accounts for <2% of AD cases (Blennow et al., 2006; Hardy and Selkoe, 2002).

Apolipoprotein E4

Over 98% of patients with AD do not have mutations in APP/Aβ processing, generally develop symptoms over age 65, and are considered to have a sporadic (also known as late onset AD [LOAD]) form of the disease (Huang and Mucke, 2012). For this group of patients, the greatest

risk factor for AD, other than age, is apolipoprotein E isoform 4 (apoE4) (Huang and Mucke, 2012). ApoE4 has been consistently identified as the major risk gene for LOAD by genome wide association studies (Bertram et al., 2010; Genin et al., 2011). The *APOE* gene has three alleles in humans: ε2, ε3, and ε4, encoding the isoforms apoE2, apoE3, and apoE4, respectively (Mahley, 1988). ApoE2 is relatively rare with an allele frequency of 7% (Mahley, 1988) and is the least studied, although it may confer protection against LOAD (Wu L and Zhao L, 2016). ApoE3 is the most common allele, with a frequency of 78%, and is considered neutral with respect to AD risk (Mahley, 1988). ApoE4 has an allele frequency of 14% (Mahley, 1988), but carriers of apoE4 account for 60–75% of AD patients. Female apoE4 heterozygotes have a 4.5-fold increased risk of developing AD compared to apoE3 homozygotes, while female apoE4 homozygotes have a 15-fold increased risk (Verghese et al., 2011; Huang and Mucke, 2012); these effects are slightly attenuated in men, who overall have a lower risk of developing AD (Raber et al., 2002). In addition to increasing lifetime risk of AD, each copy of apoE4 additionally lowers the mean age of onset by seven years for development of the disease (Farrer et al., 1997).

While the mechanism of apoE4 continues to be an active area of research, apoE4 is currently thought to act both through Aβ-dependent and –independent mechanisms (Huang and Mucke, 2012; Mahley et al., 2006). ApoE4 carriers show reduced clearance of Aβ (Kim et al., 2009), impaired neurite outgrowth (Holtzan et al., 1995), and impaired mitochondrial function (Chang et al., 2005), among other deficits. While apoE4 differs from apoE3 in only a single amino acid, this difference is enough to cause a major conformational change in the protein structure (Mahley et al., 2006) that makes apoE4 more vulnerable to cleavage by a yet-unknown protease (Brecht et al., 2004); these fragments are thought to have neurotoxic effects

(Huang, 2006). Additionally, the deleterious effects of apoE4 are upstream of Tau (Andrews-Zwilling et al., 2011); apoE4 is thus connected to both major histopathological hallmarks of AD.

Elucidation of the mechanism by which apoE4 leads to AD has been made possible by apoE4 mouse models, which capture many of the key features of human AD. The primary mouse model used by our lab is a C57Bl6J mouse line with the endogenous mouse *apoe* gene replaced with an allele of the human *APOE* gene (Hamanaka et al., 2000); these mice are referred to as apoE knock-ins (apoE-KIs). ApoE3-KI are similar to wild-type mice in most features studied. However, apoE4-KI mice show a profound age- and sex-dependent impairment in learning and memory, first emerging by ~12 months of age and becoming highly significant by 16 months (Andrews-Zwilling et al., 2012; Knoferle et al., 2014). With age, homozygous apoE4-KI female mice are more significantly impaired in learning and memory relative to homozygous apoE3-KI mice of either gender (Andrews-Zwilling et al., 2010; Leung et al., 2012). This is consistent with human data showing that female apoE4 carriers are at greater risk (Farrer et al., 1997), and for this reason we use female mice in our studies. As discussed below, several studies from our lab suggest that apoE4 causes a deficit in neuronal inhibition in the mouse hippocampus, which is responsible for the observed impairments in learning and memory.

Inhibitory-Excitatory Imbalance and Memory

Neurons receive input from both excitatory and inhibitory presynaptic inputs. Imbalance between neuronal excitation and inhibition is a key feature of several neurological diseases,

and is linked to memory impairment. An extreme example of inhibitory-excitatory (I/E) imbalance is temporal lobe epilepsy (TLE), which is known to disrupt memory (Murphy, 2013); I/E imbalance has also been observed in autism and schizophrenia (Marin, 2012; Gao and Penzes, 2015), so can be thought of as a pathological network state with a variety of disease manifestations, depending on the cell types and brain regions affected.

Experimental and theoretical work demonstrates that proper I/E balance in the hippocampus is critical for normal memory function, and that I/E imbalance impairs memory. From a theoretical perspective, efficiently storing or retrieving a memory depends on distinguishing between superficially similar inputs (Myers and Scharfman, 2009). The CA3 region is thought to be the site of pattern storage and completion in the hippocampus, and receives input from the dentate gyrus (DG) (Rolls, 2007; Rolls, 1989). The DG is thought to be the hippocampal "pattern separator", amplifying differences in signals from the entorhinal cortex and relaying these signals to the CA3 (Myers and Scharfman, 2009; Yeckel and Berger, 1990). Electrophysiological recordings of these circuits in rodents (Leutgeb et al., 2007), lesion studies (Gilbert et al., 2001), and high resolution imaging in humans during memory tasks (Berron et al., 2016), support these proposed roles for the DG and CA3. Pattern separation in the DG relies on recurrent self-loops, which are prone to runaway excitation; hence DG inhibitory interneurons are critical for efficient pattern separation and noise reduction (Myers and Scharfman, 2009; Morgan et al., 2007).

I/E imbalance is a feature of AD and is shared by both FAD and LOAD forms. Postmortem AD brains have reduced levels of GABA and GABA-producing enzymes (Zimmer et al., 1984; Jimenez-Jimenez et al., 1998). Both human AD patients and mouse models (Verret et

al., 2012) show cortical hypersynchrony and dysregulation of neural oscillations early in disease progression; early stage patients also have elevated activity (Dickerson and Sperling, 2008; Celone et al., 2006) and altered connectivity (Grecius et al., 2004) in the default mode network. Patients with mild cognitive impairment show elevated network activity that negatively correlates with hippocampal and temporal volume (Putcha et al., 2010). FAD patients commonly display epileptiform activity and full-blown epileptic seizures (Palop and Mucke, 2009). Task-related hippocampal hyperactivity is detectable by fMRI in apoE4 carriers very early in life (<30 years), long before cognitive deficits emerge (Kunz et al., 2015). Elevated hippocampal activity predicts subsequent cognitive decline in apoE4 carriers (Bookheimer et al., 2000) supporting a causative role for initial hyperactivity that eventually leads to subsequent hypofunction and neurodegeneration. A low dose of the antiepileptic drug leviteracitam was sufficient to reduce hippocampal activity of patients with mild cognitive impairment to control levels and simultaneously reverse memory deficits. (Bakker et al., 2012).

Studies from our lab have revealed that the apoE4-KI mouse model has a hippocampal-specific deficit in neuronal inhibition. ApoE4-KI mice have a selective loss of inhibitory interneurons in the hilus of the dentate gyrus (DG), which is both age- and sex-dependent (Leung et al., 2012; Andrews-Zwilling et al., 2010). Interneuron numbers are significantly lower in apoE4 mice than apoE3 mice at 16 months (Leung et al., 2012; Andrews-Zwilling et al., 2010), which is the same age that learning and memory deficits can be observed in Morris Water Maze in the apoE4 mice. The deficit in cell number and learning and memory behavior is significant only in female apoE4 mice (Leung et al., 2012), which is consistent with the observation that apoE4 is a greater risk factor in women than men. While apoE4-KI mice have impaired learning

on average, there is still individual variation in learning ability; inhibitory interneuron number in apoE4-KI mice predicts their ability to learn in Morris Water Maze (Andrews-Zwilling et al., 2010). Together these results show that learning and memory deficits are associated with inhibitory interneuron loss in the hippocampus.

Further studies from our lab have provided causal evidence connecting inhibitory interneuron dysfunction and/or loss in the hilus of the DG to learning and memory impairment. Optogenetic silencing of inhibitory interneurons in the hippocampal hilus produced transient learning and memory deficits in otherwise unimpaired wild-type mice (Andrews-Zwilling et al., 2012); therefore, inhibitory activity is necessary for spatial learning and memory. Conditional deletion of the apoE4 protein only in inhibitory interneurons rescued both cell number and learning and memory (Knoferle et al., 2014), underscoring the critical role of this cell population and demonstrating that apoE4 has cell-autonomous toxic effects on interneurons. Transplanting inhibitory interneuron progenitors into the DG of aged apoE4-KI mice functionally restored inhibition and rescued learning and memory deficits, demonstrating that restoring inhibition by replacing cells is sufficient to restore normal behavior (Tong et al., 2014). Treatment of apoE4-KI mice with the inhibition-promoting drug pentobarbital, even after interneuron loss, was also sufficient to improve learning and memory (Tong et al., 2016).

Clinical observations of AD patients reveal that the progression of cognitive impairment is not linear: despite overall decline a patient may experience fluctuations in ability (Palop et al., 2006; Bradshaw et al., 2004). Episodes of severe amnesia and disorientation are associated with epileptiform activity in EEG (Rabinowicz AL et al., 2000). This suggests that, while interneuron loss sets a ceiling on memory and cognitive function, fluctuations in network

activity also constrain cognitive performance (Palop and Mucke, 2009). Thus, modulating neuronal inhibition, even without increasing interneuron number, could be an effective symptomatic treatment (Palop and Mucke, 2009).

Could increasing neuronal inhibition have disease-modifying effects as well? Multiple lines of evidence suggest that this is the case. In the apoE4-KI model, early short-term treatment with pentobarbital (i.e. before substantial cellular loss) prevented neuronal losses and learning and memory deficits when the mice were evaluated months later (Tong et al., 2016). Hippocampal hyperactivity is a risk factor for AD, and reducing this activity could therefore halt disease progression. Excitotoxicity is a plausible mechanism for this disease modification (Hynd et al., 2004); increasing neuronal inhibition could rebalance the network and arrest cell death (Ong et al., 2013). Consistent with this, treating apoE4-KI mice with pentobarbital before interneuron losses occurred prevented those losses and resulting learning and memory deficits (Tong et al., 2016). Treating inhibition itself as a therapeutic target respects the multifactorial nature of AD; hyperexcitability is a feature of both FAD and LOAD and associated mouse models (Huang and Mucke 2012). Aβ production itself is causally linked to neuronal activity, as neuron firing leads to changes in protein trafficking that favor proteolytic cleavage of APP into Aβ (Das et al., 2013). Although it has been suggested that increased excitation, rather than decreased inhibition, may be a feature of mouse FAD models in contrast to apoE4 models (Palop et al., 2007), increasing inhibition would shift the network toward a balanced state regardless of the initial cause of the disruption. We may remain agnostic on the amyloid hypothesis, or indeed any major proposed causal mechanism for AD, and still regard neuronal inhibition as an effective target.

GABAergic Transmission

Gamma-aminobutyric acid (GABA) is the main inhibitory neurotransmitter in the brain. Neurons have both ionotropic and metabotropic receptors for GABA, which are referred to as $GABA_A$ and $GABA_B$ receptors, respectively. GABA binding causes a conformational change in $GABA_A$Rs which opens an ion pore and allows the movement of chloride (and to a lesser extent, bicarbonate) anions through the cell membrane (Korpi et al., 2002). The equilibrium potential for GABA (E_{GABA}) depends both on the membrane potential of the cell and the driving force for chloride flux (E_{Cl}); in mature neurons, the potassium-choride cotransporter KCC2 maintains an E_{Cl} that is more negative than the resting potential of the cell, so E_{GABA} is also negative (Luscher et al., 2011; Farrant and Nusser, 2005). In this case, GABA binding then causes influx of anions and hyperpolarization, which renders most neurons less likely to fire an action potential (Farrant and Nusser, 2005). Alterations in E_{Cl} can affect E_{GABA} and depress inhibition; as discussed below, this is indeed a feature of many disease states.

$GABA_A$Rs are heteropentamers composed of five subunits drawn from at least 19 possible types (Whiting, 2003). While the combinatorial possibilities of $GABA_A$R composition are enormous, in the brain only a small number (perhaps 25) (Seymour et al., 2012) of these possible receptors are expressed. The archetypal $GABA_A$R contains two α subunits (of types 1-6), two β subunits (of types 1-3), and one additional subunit, typically either γ2 or δ (Whiting PJ, 2003). The minimal requirement for a $GABA_A$R *in vivo* is a pentamer built from α and β subunits, and the interface between these two subunits forms the GABA binding site (Sieghart and Sperk, 2002). Other subunits, however, can influence binding at the GABA site: the δ

subunit, for example, confers five-fold higher binding affinity for GABA (Mortensen and Smart, 2006). Different subunits also confer distinct localization of the $GABA_AR$ within the membrane. By interacting with the synaptic anchoring proteins gephyrin and GABARAP, γ2 targets the $GABA_AR$ complex to synaptic sites (Mody, 2001; Korpi et al., 2002). By contrast, δ-containing receptors are found exclusively at peri- and extra-synaptic sites, where they respond to 'spillover' GABA that diffuses from synaptic (Wei et al., 2003) and glial (Mody, 2001) sources. One notable exception to these rules is the α5βγ2 receptor, which is also generally extrasynaptic and is functionally similar to the δ-containing receptor (Mody, 2001). Additionally, different subunits are restricted to particular regions of the brain or even subregions of the same structure; for example, α4βδ receptors are predominantly expressed in DG granule cells (Wei et al., 2003) while α5βγ2 receptors are found in the CA3 region of the hippocampus (Mortensen and Smart, 2006).

Neurophysiologists distinguish between two forms of neuronal inhibition: phasic and tonic. Phasic inhibition is transiently generated by an action potential in a presynaptic inhibitory interneuron; phasic inhibition is observed in all neurons and brain regions, is necessary for neuronal oscillations, and involves the brief and near-simultaneous opening of many $GABA_ARs$ (Farrant and Nusser, 2005). By contrast, tonic inhibition is the baseline holding current required to clamp a neuron at a given potential; it is a stable, continuous form of inhibition that does not depend on action potentials (Mody, 2001; Farrant and Nusser, 2005). Tonic inhibition is not observed in all neurons or brain regions, but is a well-established feature of neurons in the cerebellum (Mody, 2001; Ye et al., 2013) and hippocampus (Farrant and Nusser, 2005; Petrini et al., 2004).

Pharmacological and genetic studies have revealed that distinct populations of $GABA_AR$s mediate these two forms of inhibition: while synaptic $GABA_AR$s mediate phasic inhibition, extrasynaptic receptors mediate tonic inhibition (Mody, 2001). This is reflected in the unique properties of extrasynaptic receptors: very high affinity for even ambient GABA, as well as low or absent desentization to repeated GABA exposure (Mody, 2011; Mortensen and Smart, 2006). Through a variety of mechanisms, including altering membrane potential and increasing membrane conductance (i.e. shunting inhibition) (Walker and Kullmann, 2012), these extrasynaptic $GABA_AR$s set the excitability threshold of entire neural circuits.

However, tonic inhibition does not simply silence neuronal signaling; there is considerable evidence that increased tonic inhibition stabilizes circuits and increases their signal-to-noise ratio (Walker and Kullman, 2012). Consistently, seizure risk is attenuated during pregnancy and certain points of the menstrual cycle; during times of reduced seizure probability, neurosteroids potentiate function of δ (Belelli and Lambert, 2005; Maguire et al., 2005) and/or upregulate expression of its partner α4 (Smith et al., 2007; Maguire and Mody, 2009). Neurons actually shift $GABA_AR$s from the synaptic to the extrasynaptic zone as a protective mechanism against seizures (Zhou et al., 2013), underscoring the critical role of tonic inhibition for circuit stability. The stabilization effect of tonic inhibition is likely a joint product of the much larger inhibitory charge transfer mediated through tonic vs. phasic inhibition (Glykys et al., 2008) as well as the ability of tonic conductance to *enhance* the firing of interneurons in some cases (Song et al., 2011). Intriguingly, pentobarbital, which restores L/M in apoE4-KI mice (Tong et al., 2016), has a stronger effect at extrasynaptic receptors despite an apparent lack of pharmacological specificity (Feng et al., 2004) this is probably due to the fact

that GABA is only a partial agonist at these receptors (Jensen et al., 2013) giving them greater dynamic range for positive modulation. Additionally, benzodiazepines -- which act at synaptic receptors -- increase risk for dementia (de Gage et al., 2012), further arguing for tonic, not phasic, inhibition as a target for improving L/M.

Extrasynaptic $GABA_AR$s, which mediate tonic inbibition, have region- and even subregion-specific patterns of expression in the brain. As the apoE4-KI model of AD shows interneuron losses in the hilus of the hippocampus, a hilar extrasynaptic $GABA_AR$ would be a promising target for restoring inhibition in this model. As discussed, δ is expressed most highly in dentate gyrus granule cells (in partnership with α4) (Wisden et al., 1992; Pirker et al., 2000) and mediates the majority of tonic inhibition there (Chandra et al., 2006; Glykys J et al., 2008; Herd MB et al., 2008). Consistently, knockout mice for δ show dramatically reduced tonic inhibition (Spigelman et al., 2003; Glykys et al., 2008), greater seizure risk (Olsen et al., 1997), and some L/M deficits at young age (Whissell et al., 2013), though no studies have examined these mice at advanced age. Intriguingly, expression of δ is downregulated in postmortem AD brains (Berchtold et al., 2013), suggesting that loss of this protein may contribute to I/E imbalance in AD.

Chloride Cation Cotransporters Establish Chloride Equilibrium

The hyperpolarization of a mature neuron in response to GABA depends on maintenance of a chloride gradient, with relatively high chloride outside the cell (Payne et al., 2003). A family of proteins, the chloride cation cotransporters (CCCs), actively transport chloride across the plasma membrane to maintain this gradient. In humans, there are 9 members of the CCC family

(Blaesse et al., 2009). While CCCs are expressed in every tissue type, phylogenetic evidence suggests that their role in maintaining chloride gradients in the brain is the most evolutionarily ancient function of CCCs (Hekmat-Scafe et al., 2006).

The chloride gradient in neurons is maintained chiefly by two CCCs: sodium-potassium-chloride cotransporter 1 (NKCC1) and potassium-chloride cotransporter 2 (KCC2). NKCC1 imports chloride into the cell, while KCC2 exports chloride (Blaesse et al., 2009). The relative expression of these two proteins determines E_{Cl} and thus E_{GABA}, with KCC2 promoting GABA-induced hyperpolarization of the neuron and NKCC1 attenuating hyperpolarization or even promoting GABA-induced depolarization (Ye et al., 2012; Kahle et al., 2008). KCC2 deficient mice display depolarized E_{GABA}, seizures, and early postnatal death (Tornberg et al., 2005). Efficient neuronal inhibition depends on a low ratio of NKCC1:KCC2 (Blaesse et al., 2009).
In neurons, CCCs are developmentally regulated. In immature neurons, the ratio of NKCC1:KCC2 expression is high, while the opposite is true in mature neurons; E_{GABA} becomes more negative as neurons mature, reflecting a higher internal chloride concentration (Payne et al., 2003). The transition from higher NKCC1 to KCC2 expression is precisely timed and is called the "developmental switch". The timing is species-specific; in rodents, the switch begins after birth and completes by postnatal day 21, while in humans it begins before birth and proceeds over the first year of life (Dzhala et al., 2005). The exact mechanism of the switch is unknown, although it has been argued that KCC2 itself suppresses NKCC1 expression (Frederikse and Kasinathan, 2015). Proposed mechanisms for the initial upregulation of KCC2 include developmental release of a suppressive factor (Yeo et al., 2009) and GABA-induced signaling cascades (Ganguly et al., 2001).

Alterations in CCC expression occur in many neurological disease states. NKCC1 is upregulated and KCC2 is downreglulated (Aronica et al., 2007) in the hippocampus in humans with TLE (Palma et al., 2006; Sen et al., 2007; Shimizu-Okabe et al., 2007) and various rodent models of TLE (Brandt et al., 2010; Pathak et al., 2007). Increases in the ratio of NKCC1:KCC2 expression have also been implicated in autism (Ben-Ari et al., 2015), chronic pain (Kaila et al., 2014), and Down syndrome (Deidda et al., 2015). The net effect of these changes to CCCs in these disease states is to shift neurons toward an immature state with depolarized E_{GABA} (Kahle et al., 2008). Delay in the developmental switch itself is a feature of Fragile X syndrome (See He et al., 2014) and schizophrenia (Hyde et al., 2011). Due to their connection to disease states and role in maintaining neuronal inhibition and E_{GABA}, CCCs have been considered attractive drug targets.

Bumetanide

Bumetanide is a small molecule that is approved by the Food and Drug Administration (FDA) as a treatment for edema (Puskarjov et al., 2014; Brater et al., 1984). It is widely recognized as a specific inhibitor of the ubiquitous CCC NKCC1 and the kidney-specific CCC NKCC2, with no reported effects on other CCCs (Hasannejad et al., 2004). Early work revealed that bumetanide alters osmotic balance in loop of Henle in the kidney, leading to diuresis (Bourke et al., 1973; Imai, 1977). Evidence that bumetanide targets NKCC1 was first provided by *in vitro* studies demonstrating that the compound reduces chloride influx but does not affect outflux, and that it reduces membrane transport of sodium and potassium ions in addition to chloride (McGahan et al., 1977). Changing the chloride concentration itself shifts the dose-response curve for

bumetanide, which suggests that, at least in part, bumetanide acts as a competitive inhibitor of NKCC1 at the chloride site (Haas and McManus, 1983). The effects of bumetanide are abolished in NKCC1 knockout mice, confirming its specificity within the brain (Dzhala et al., 2005; Flagella et al., 1999).

Consistent with its role as an NKCC1 inhibitor, bumetanide alters chloride homeostasis in neurons and thereby induces a negative shift in E_{GABA}. *In vitro* slice physiology recordings from CA1 (Dzhala et al., 2005; Dzhala et al., 2007) and CA3 pyramidal cells (Nardou et al., 2009) in the hippocampus consistently show that application of bumetanide causes a negative (hyperpolarizing) shift in E_{GABA}, via altered E_{Cl^-} (Deidda et al., 2015). Bumetanide's protective effects in TLE are abolished by the $GABA_AR$ antagonist bicuculline, suggesting that bumetanide functionally promotes inhibition *in vivo* (Dzhala et al., 2005).

Due to its effects on chloride balance, bumetanide has been pursued as a treatment for neurological disease in animal models and human trials. Behavioral and/or functional rescues have been obtained from rodent models of TLE (Dzhala et al., 2005; Dzhala et al., 2007; Brandt et al., 2010), Down syndrome (Deidda et al., 2015), and Parkinson's disease (Dehorter et al., 2012). Bumetanide is not a panacea; notably a trial for human infantile epilepsy was not successful (Ben-Ari et al., 2016), possibly due to bumetanide interfering with the developmental role of NKCC1 (Wang and Kriegstein, 2011). However, in trials for human patients beyond infancy, bumetanide treatment has yielded promising results, e.g. for autism (Hadjikhani et al., 2015; Lemmonier et al., 2012), Parkinson's disease (Damier et al., 2016), and schizophrenia (Lemmonier et al., 2016).

An examination of bumetanide's pharmacology reveals both strengths and weaknesses for clinical use. Bumetanide is a potent NKCC1 inhibitor with a reported half-maximal inhibitory concentration (IC_{50}) of 100-500nM (Puskariov et al., 2014; Suvitayavat et al., 1994; Beck et al., 2003). However, it has a short half-life of ~1 hour in humans (Pentikäinen et al., 1977) and ~30 minutes in rodents (Cleary et al., 2013; Lee et al., 1994). Additionally, bumetanide is poorly bioavailable, with roughly 1:100 brain:plasma ratio (Cleary et al., 2013). Despite these drawbacks, even low doses of bumetanide administered systemically, e.g. 0.2 mg/kg by intraperitoneal injection, have both acute and disease-modifying effects (Sivakumaran and Maguire, 2015; Brandt et al., 2010) in TLE models. Since systemic administration and direct hippocampal infusion of bumetanide both suppressed kainic acid seizure kindling with equal efficacy, bumetanide appears to reach and act on the hippocampus even at low systemic doses (Sivakumaran and Maguire, 2015).

Hypothesis to Be Tested

Inhibitory dysfunction is a feature of AD in patients and our apoE4-KI model, which shows substantial loss of inhibitory interneurons in the DG of the hippocampus. Past work from our lab showed that replacing these lost interneurons with transplanted progenitor cells rescued L/M. I hypothesize that restoring postsynaptic inhibitory transmission, rather than presynaptic inhibitory input, would also rescue L/M in our apoE4-KI model.

Here we demonstrate that apoE4-KI mice (1) have an age-dependent increase in NKCC1:KCC2 expression; (2) that systemic bumetanide treatment rescues L/M in aged apoE4-KI

mice; and (3) that overexpression of GABAAR subunit δ in the DG of aged apoE4-KI mice rescues L/M and restores interneuron numbers.

CHAPTER 2

Materials and Methods

Animals

All protocols and procedures followed the guidelines of the Laboratory Animal Resource Center at the University of California, San Francisco (UCSF). Experimental and control animals had identical housing conditions from birth through death (12-hour light/dark cycle, housed 5/cage, PicoLab Rodent Diet 20). All mouse lines were maintained on a C57Bl/6J background strain. ApoE3-KI and apoE4-KI homozygous mouse lines (Taconic) (Hamanaka et al., 2000) were born and aged under normal conditions at the Gladstone Institutes/UCSF animal facility. All mice are female; ages of mice used are indicated for each study. Deletion of apoE4 in forebrain interneurons was achieved by crossing LoxP-floxed apoE knock-in mice (apoE-fKI) (Bien-Ly et al., 2012) with Dlx-Cre transgenic mice [B6.Cg-Tg[Tg(I12b-cre) 671Jxm/J] (Potter et al., 2009).

Pentobarbital Treatment

Pentobarbital was prepared at 5 mg/mL in 0.9% sterile saline. Injections were given daily, i.p., for 14 days at a volume producing an overall dose of 20mg/kg. Controls were injected with a matching volume of 0.9% sterile saline. Strong sedative effects, including slowed/uncoordinated movement and sleep, were observed acutely (<5 minutes) after injection. After the two-week injection period brain tissue was collected and prepared for Western Blotting.

Bumetanide Treatment

Bumetanide was prepared at 220uM (High Bumetanide) or 22uM (Low Bumetanide) in 2% DMSO in 0.9% sterile saline, and adjusted to pH 8.5 with NaOH for solubility. Injections were given daily, i.p., for 30-60 days preceding behavioral assessment (timeline indicated for each cohort), and continuing throughout behavioral assessment. Weight was measured weekly for each mouse, and injection volume was calculated to achieve a dose of 0.2 mg bumetanide / kg body mass (High Bumetanide) or 0.02 mg bumetanide / kg body mass (Low Bumetanide) (e.g., 50uL daily injection for a mouse weighing 20g). Control mice were injected with a matched volume of 2% DMSO in 0.9% sterile saline, pH 8.5. Injections were well tolerated and no adverse health effects were noted.

Behavioral Tests

Behavioral tests were performed for bumetanide-treated mice after no fewer than 30 days of treatment, up to as many as 100 days (see experimental timelines for each cohort). Bumetanide treatment was continued during behavioral tests; injections were administered at the end of the light cycle and after the day's test was concluded.

For mice overexpressing δ, behavioral tests were conducted 30 days following lentiviral injection (see below), and carried out over a 60-day period.

Prior to behavioral tests, mice were singly housed. Each mouse was assigned a random number to mask their genotype and treatment information; in the bumetanide studies, an

investigator would be unblinded to the treatment at the conclusion of each trial day so the injection could be administered.

Morris Water Maze (MWM) is a common measure of spatial learning and memory behavior in rodents and is known to be hippocampus-dependent (Morris, 1984; Vorhees and Williams, 2006). The mouse is placed into a pool of opaque water and must use large spatial cues placed on the walls to navigate to a hidden platform, where it is rewarded by being removed from the pool. If the mouse fails to find the platform within 60 seconds, the experimenter guides the mouse to the platform, allows the mouse to sit for five seconds, then removes the mouse from the pool. The mouse is evaluated in four trials per day for 5 days; learning is measured by the improvement in escape time as a function of hidden day number. The pool is a 122 cm diameter round tank filled with room temperature water. A 10 cm^2 platform is submerged 1.5 cm below the surface of water, and the water is made opaque with one bottle white Powder Tempra Paint (Discount School Supply #CPTWH) during hidden trials. Mice were allowed 48 hours to habituate to the testing room prior to MWM and were pre-trained 24 hours before MWM to familiarize the animals with the submerged platform and the task. Throughout MWM, performance was monitored and quantified using Etho-Vision motion tracking software (Noldus Information Technology).

During the MWM experiment, mice were trained to locate the hidden platform over 4 trials per day for 5 days (H1-5), where H0 was the first trial on H1. The cohort was divided into sub-groups of 10-15 mice and each sub-group swam two consecutive trials before the next sub-group swam. Each sub-group rested approximately 3 hours between sessions, swimming two sessions per day and two trials per session.

After completing hidden trials, memory performance was assessed through probe trials. Each probe trial was conducted for 60 seconds in the absence of the platform at 24, 72, and 120 hours after the final learning session. Probe trials are quantified by measuring the amount of time the mouse spends in the quadrant that formerly held the platform ("target quadrant"); preference is assessed by comparing the percent of total time the mouse spent in the target quadrant versus the mean of the other three quadrants ("off-target quadrants").

Following the probe trials, visible trials were conducted. In these trials, the platform was marked by a 15cm tall black-and-white striped mast, and placed in each of the three quadrants not used in the hidden trials. As in the hidden trials, mice were assessed by the length of time required to find the platform.

Cognitive flexibility and re-learning can be assessed through a modified form of MWM – reversal MWM (Vorhees and Williams, 2006). In reversal MWM, mice must learn the location of a hidden platform, then adapt to a new platform location. Mice are trained to locate a hidden platform over a period of days, as in standard MWM, and are then assessed for target quadrant preference in a single probe trial at 24 hours following the final hidden day. Then the platform is placed back into the pool, but at a new location – typically in the opposite position as the original (i.e., 180 degrees around the pool). Then, mice are trained to find the new platform location using a standard hidden training methodology, followed by probe and visible trials.

Open field test assesses habituation and activity behavior by allowing the mice to explore a novel, empty environment (Gould et al., 2009). After 2 hours of room habituation, mice were placed in an odor-standardized chamber for 15 minutes. Behavior was objectively

analyzed by software from San Diego Instruments. The maze was thoroughly cleaned with 30% ethanol between trials.

Elevated plus maze evaluates anxiety and exploratory behavior by allowing mice to explore an open, illuminated area (open arm) or hide in a dark, enclosed space (closed arm), both suspended 63 cm above the ground (Walf and Frye, 2007). After 2 hours of room habituation in dim light, mice were placed in an odor-standardized maze at the junction of the open and closed arms. Behavior was analyzed by infrared photo-cells interfacing with Motor Monitor software (Kinder Scientific), and quantified for the time spend in open and closed arms. The maze was thoroughly cleaned with 30% ethanol between trials.

Rotarod objectively evaluates stamina, coordination, and movement behavior (Jones et al., 1968). During the test, mice are placed on a 3cm diameter plastic rod, supported 30 cm above the base of the machine. The rod is scored with parallel ridges that allow the mouse to grip the rod effectively. The rod is then rotated with slowly increasing angular velocity, and either latency to falling off the rod or final angular velocity of the rod can be used as proxies for stamina. The elevation of the rod provides motivation for mice to participate in the task; the time of falling is determined using the break in an infrared beam running along the bottom of the apparatus. In case the mouse stops running and simply grips the rod as it spins, the trial is concluded if the mouse rotates with the rod three times.

On the first day of Rotarod, mice are trained to understand the task by being placed on the rod at constant 16 RPM for 3 5-minute sessions with a 5-minute rest between each trial. This training day is not used for evaluation. Then, on the second and third days, the rod is

accelerated from 4-40 RPM at 7.2 RPM/minute and reaches maximum speed at 5 minutes; the trial is concluded if the mouse falls, if the mouse does not fall but rotates with the rod 3 times, or after 5.5 minutes. Two blocks of three sessions are performed each day, with 5 minutes between each session and 1.5 hours between each block.

Viral Vectors

Viral expression of δ and GFP *in vivo* was achieved via a lentiviral expression vector (FUW_GFP-furin-V5-p2A-TGA, 11.5 kB backbone), which was obtained from Michael Ward in the Li Gan lab. The vector uses a ubiquitin promoter to drive expression of an EGFP-Furin-V5 construct, which is separated from the target gene with a self-cleaving p2A peptide, allowing 1:1 expression of GFP to the target gene (Yang et al., 2008). Lentivirus was chosen for delivery of the target gene because it can infect and integrate genetic material into non-dividing cells, such as neurons. For the GFP-only vector, the backbone was left unmodified, and a stop codon follows the p2A peptide. The human gene encoding for δ, *GABRD,* was subcloned into the backbone following the p2A at an RsrII restriction site, and site-directed mutagenesis was used to trim away the restriction site and leading stop codon. Insertion of *GABRD* was confirmed via sequencing (Elim Bio). The vector was grown using competent *E. Coli* and selected via ampicillin resistance. Expression vectors were packaged into lentivirus, concentrated, and titered by the UCSF ViraCore. GFP-only vector was concentrated to a final titer of 7.6×10^7 viral particles / mL, while δ vector was concentrated to a final titer of 3.1×10^7 viral particles / mL.

Hippocampal Injection

For in vivo expression of GFP or GFP/δ, 6 x 10^4 viral particles were injected bilaterally into the hippocampus. Virus was loaded into gauge 33 stainless steel cannulae (Plastics One) connected to thin wall plastic tubing (Plastics One). Tubing was initially backfilled with mineral oil (Sigma) on a Nanoject II (Drummond Scientific Company); virus was pipetted onto DuraSeal stretch film (Sigma) and drawn through the cannula into the tubing using the Nanoject motor. The coordinates for injection into the dentate gyrus were X = ±1.5, Y = -2.1, Z = -2.1, measured in mm from the surface of the brain (for Z) and the bregma point on the skull (for X and Y) (Lein et al., 2007). Surgery was performed on a Kopf Small Animal Frame 940 with Model 943 ear bars (David Kopf Instruments).

Mice were anesthetized with 100uL ketamine (10 mg/mL) and xylazine (5 mg/mL) in 0.9% saline (Hospira) by i.p. injection and maintained on 0.8-1% isoflurane (Harry Schein) in 1.5 L/min O_2 (Laboratory Animal Resource Center, UCSF). Respiratory rate was monitored throughout the procedure; if breathing became labored, shallow, or excessively slow, isoflurane concentration was reduced.

Prior to surgery, I removed hair from the mouse's skull using Nair (Church & Dwight). I applied Puralube veterinary ointment to the mouse's eyes to prevent drying (Dechra). I placed the mouse into the stereotactic frame and applied gentle pressure to ensure that the head was stable. I confirmed anesthesia using the toe pinch reflex, then made an incision through the skin covering the center of the skull using a scalpel and sterilized the incision site with 10% hydrogen peroxide. I drilled holes through the skull (but not the dura) using a 0.5mm microburr

(Fine Science Tools), then hand-punctured the dura with a metal needle. At each site, viral particles were infused at 100nL/min for 10 minutes and allowed to diffuse for 5 minutes before withdrawing the cannulae. During recovery, I gave mice 1.5 L/min O_2 for 10 minutes and sutured the incision with monofilament non-absorbent nylon sutures (Ethicon). While the mice were still anesthetized, I administered the analgesics ketophen (100uL at 1 mg/mL) in saline (subcutaneous between shoulders) and buprenorphine (100uL at 7.5 ug/mL) in saline (i.p.). Mice were placed into an empty cage, with half the cage on a heating pad, until ambulatory (generally ~2 hours). Feed and a hydrating gel pack were placed onto the cage floor during recovery to minimize the need for mice to crane their heads in order to eat and drink. For follow-up care, mice were monitored daily for signs of pain (e.g. hunching, slow movement), and given additional injections of analgesic daily until signs of pain were no longer evident.

Western Blotting

Mice were transcardially perfused with 0.9% saline (w/v) and hemibrains were collected and snap-frozen in ethanol on dry ice. Hippocampus was dissected using forceps on ice. Hippocampal tissue was homogenized on ice – 5 times for 30 seconds each, with 30 seconds between homogenizations – in high detergent buffer (HDB) (50mM Tris, 150 mM sodium chloride, 2% NP40, 1 % sodium deoxycholate, 4% SDS, and 2 pellets Complete protease inhibitor cocktail [Roche] in 50mL deionized water). Samples were spun at 30,000 rpm for 30 minutes at 4°C in a tabletop centrifuge, and the protein supernatant was saved. Protein concentration was measured using the Pierce BCA Protein assay (Thermo Scientific) using the microplate procedure and quantified on a FlexStation II plate reader (Molecular Devices).

Protein concentration was adjusted to 2 ug/uL in HDB, distributed into 60ug aliquots, and stored at -80°C for later use.

For Western blotting, samples were prepared by mixing 30ug protein with 7uL loading buffer, then incubating for 10 minutes at 70°C in a PCR machine. Loading buffer was NuPage 4X LDS sample buffer (Invitrogen) mixed 2.5:1 with NuPage sample reducing agent (Invitrogen). Protein samples were run on NuPage Bis-Tris gels, either 12% or 4-12% gradient (Invitrogen), as indicated in the text. Gels were inserted into an Xcell SureLock mini-cell electrophoresis system (Invitrogen) and protein was loaded at 30ug/well in a total volume of 15uL. The electrophoresis box was filled with MOPS buffer (Invitrogen) and 0.5 mL NuPage antioxidant was added into 200mL MOPS in the upper chamber only. ProteinPlus kaleidoscope was used as the molecular weight marker (Bio-Rad). Since I observed that the leftmost and rightmost lanes tended to cause smearing in the protein bands, these lanes were left unused when possible.

Protein was slowly run from the well into the gel at 120 V for 10 minutes, then the voltage was increased to 200 V for 50-60 minutes to separate proteins. After separation was complete, gel was removed from the electrophoresis box and inserted into a sandwich of extra thick blot paper (Bio-Rad) soaked in semi-dry transfer buffer, and a nitrocellulose membrane with 0.45uM pore size (Invitrogen). Protein was transferred to the membrane using a Trans-Blot Turbo transfer system (Bio-Rad) at 18V for 1 hour. After transfer, success was checked using a Ponceau stain and photographed, and stain was washed off using deionized water and PBS. Nonspecific binding was blocked using PBS blocking buffer (Li-Cor) for 1 hour. Primary antibody was diluted in PBS blocking buffer and membrane was incubated in primary solution overnight

(18-20 hours) on a rocker at 4°C; see Table 1A for primary antibodies used. Primary solution was washed using 0.5% Triton-X in PBS (PBST), then secondary antibody was prepared in PBS blocking buffer and membrane was incubated for 1 hour at room temperature; see Table 1B for secondary antibodies used. Secondary solution was washed using PBST, then membrane was stored in PBS until imaging.

Blots were imaged on an Odyssey scanner (Li-Cor) and quantified using Image Studio Lite software (Li-Cor). Image processing was performed in Photoshop (Adobe) to enhance contrast and alter image brightness for better print image quality; in these cases, the alteration was performed on the full blot. The original, unaltered image was always used for quantification.

Table 1. Antibodies used for Western Blotting

A. Primary Antibodies

Host	Target	Concentration	Manufacturer	Catalog #
rabbit	anti-NKCC1	1:333	Abcam	ab59791
rabbit	anti-KCC2	1:1000	Abcam	ab49917
mouse	anti-GAPDH	1:2500	Millipore	MAB374
rabbit	anti-GABRD, N-terminal	1:200	Novus	NB300-200
mouse	anti-beta actin	1:1000	Abcam	ab8226

B. Secondary Antibodies

Host	Target	Concentration	Manufacturer	Catalog #
IRDye 800CW donkey	mouse,	1:10000	LiCor	925-32212
IRDye 680RD donkey	mouse	1:10000	LiCor	925-32213
IRDye 800CW donkey	rabbit	1:10000	LiCor	925-68072
IRDye 680RD donkey	rabbit	1:10000	LiCor	925-68073

Immunohistochemistry

Mice were transcardially perfused with 0.9% saline (w/v) and hemibrains were collected and drop-fixed in 4% paraformaldehyde (PFA) for 24 hours at 4°C. After rinsing in PBS, tissue was cryoprotected in 30% (w/v) sucrose and sectioned coronally (30 µm) with a frozen sliding microtome (Leica) for floating section immunohistochemistry. Brain sections were stored in cryoprotectant medium (30% glycerol and 30% ethylene-glycol in PBS) at -20°C prior to staining.

For fluorescent staining, sections were first washed 3 times in PBS to remove cryoprotectant medium, then permeabilized in PBST for 30 minutes at room temperature. Nonspecific binding was blocked for 1 hour at room temperature using blocking buffer (10% normal donkey serum and 0.2% gelatin in PBST) before primary incubation overnight on a rocker at 4°C in primary solution (3% normal donkey serum, 0.2% gelatin, and primary antibodies in PBST); see Table 2A for a list of primary antibodies used. Secondary antibodies were prepared in secondary solution (3% normal donkey serum and 0.2% gelatin in PBST) and incubated for 1 hour at room temperature in the dark; see Table 2B for a list of secondary antibodies used. Sections were mounted onto glass slides in PBS, dried, then coverslipped in Vectashield antifade mounting medium for fluorescence (Vectorlabs). Coverslips were sealed with clear nail polish.

For DAB staining, sections were washed three times in PBS to remove cryoprotectant medium, then citrate antigen retrieval was used to disrupt PFA crosslinking to allow better access to antigens. Sections were placed into citrate buffer (9 parts water + 1 part [9 parts 0.1M sodium citrate + 1 part 0.1M citric acid]) at 95°C, then cooled to room temperature. Sections

were permeabilized in PBST for 30 minutes at room temperature. Endogenous peroxidase activity was blocked using a solution of 3% hydrogen peroxide and 10% methanol in PBS for 15 minutes. Nonspecific binding was blocked for 1 hour in blocking buffer (10% normal goat serum, 1% blotting grade blocker non-fat dry milk [Bio-Rad] and 0.2% gelatin [Sigma] in PBST). Primary antibody stain was performed overnight (18-22 hours) at 4°C on a rocker in primary buffer (3% normal goat serum, 0.2% gelatin and primary antibodies in PBST). Sections were incubated for 90 minutes in secondary antibody buffer (3% normal goat serum, 0.2% gelatin and biotinylated secondary antibodies in PBST). Avidin-Biotin Complex (ABC) solution (4.5uL/mL avidin and 4.5uL/mL biotin in PBST, ABCVectorElite) was prepared 30 minutes before use, and sections were incubated in ABC for 1 hour. Sections were washed in PBST, PBS, then 0.1M Tris buffer, pH 7.4, then antigen was stained to a brown color using DAB solution (1x DAB, 0.1M Tris buffer, and 0.01% hydrogen peroxide) for 2-5 minutes, until sections were visibly brown. Color-change reaction was stopped using Tris buffer. Sections were mounted in gelatin on glass coverslips, which were left to dry overnight, then dehydrated with xylene 2x for 10 minutes each. Sections were coverslipped in Cytoseal mounting media (Thermo Scientific).

Table 2. Antibodies used for Immunohistochemistry

A. Primary Antibodies

Host	Target	Concentration	Manufacturer	Catalog #
rabbit	anti-NKCC1	1:333	Abcam	ab59791
rabbit	anti-KCC2	1:333	Abcam	ab49917
mouse	anti-MAP2	1:1000	Millipore	MAB3418
goat	anti-GFP	1:500	Abcam	ab6673
rabbit	anti-GABRD, N-terminal	1:200	Novus	NB300-200
rabbit	anti-somatostatin	1:250	Millipore	MAB354

B. Secondary Antibodies

Host	Target	Concentration	Manufacturer	Catalog #
Alexa Fluor 488 donkey	anti-rabbit	1:1000	Life Technologies	A-21206
Alexa Fluor 488 donkey	anti-goat	1:1000	Life Technologies	A-11055
Alexa Fluor 594 donkey	anti-rabbit	1:1000	Life Technologies	A-21207
Alexa Fluor 594 donkey	anti-mouse	1:1000	Life Technologies	A-21203
biotinylated goat	anti-rabbit	1:250	Vector Laboratories	BA-1000

Image Collection and Quantification

Brain sections were imaged on a Keynce BZ-9000 tabletop microscope. Imaging parameters were kept constant across sections and brains to allow accurate quantification. Fluorescence images were captured at 20x in both red and green channels, with an exposure time of 1/20s and 1/9s, respectively.

Image fluorescence was quantified using ImageJ software. A highlighted region of fixed size was chosen within the hilus, CA1, or CA3, and average fluorescence intensity across the region was quantified with ImageJ software (National Institutes of Health) then averaged across genotype.

DAB staining for somatostatin-positive interneurons was quantified by manually counting positive cells in brightfield images. Since every 10^{th} section was saved during the sectioning procedure, total cell number across the hippocampus was extrapolated by multiplying the counted cells by 10. 7 sections were counted from each animal; in the cases where more than 7 sections were available across the hippocampus, a set of 7 images was chosen to give a similar representation along the rostral-caudal axis for all mice. The experimenter was blinded to the genotype and treatment of the mouse during counting.

Statistical Analysis

Values are expressed as mean ± standard error. Differences between means were assessed by Student's *t* test or analysis of variance (ANOVA) using Excel (Microsoft). Least-squares linear regression was performed in Python using the scipy.stats.linregress package. For

immunohistochemistry, channel coherence was measured using Pearson's R with the Fiji software package Coloc 2 (Costes 2004). $P < 0.05$ was considered statistically significant. In plots, a single asterisk (*) denotes a significant difference with $p < 0.05$, while two, three, and four asterisks indicate significant differences with $p < 0.01$, 0.001, and 0.0001, respectively.

CHAPTER 3

Chronic Bumetanide Treatment Restores Learning and Memory in ApoE4 Knock in Mice

Altered CCC Expression Is a Novel Age- and ApoE-dependent Phenotype

An imbalance in NKCC1:KCC2 has been implicated in several neurological disease states, including TLE, Down syndrome, schizophrenia, and others. Therefore, I used Western blotting to assess whether the expression of NKCC1 and/or KCC2 differed in apoE3- and apoE4-KI mice. We considered three time points: early adulthood (2 MO), middle adulthood (10 MO), and old age (18 MO); learning and memory deficits and interneuron losses emerge by 12-16 MO in the apoE4-KI model. At each timepoint, hippocampal tissue was collected from apoE3- and apoE4-KI female mice and probed for NKCC1 and KCC2 (see Methods); as NKCC1 is expressed in many cell types, GAPDH was used as a total protein control.

2 MO apoE3- and apoE4-KI mice did not differ in NKCC1 expression normalized to GAPDH (NKCC1:GAPDH) (E3-KI: 0.0052±0.00079; E4-KI: 0.0042±0.00046; $p = 0.29$), KCC2 expression normalized to GAPDH (KCC2:GAPDH) (E3-KI: 0.033±0.0015; E4-KI: 0.033±0.0043; $p = 0.98$), or NKCC1:KCC2 ratio (E3-KI: 0.16±0.019; E4-KI: 0.13±0.019; $p = 0.39$) (Fig. 1A), as measured on 4-12% Bis-Tris gradient gels. n = 4 for apoE3-KI and 4 for apoE4-KI.

10 MO apoE3- and apoE4-KI mice did not differ in NKCC1:GAPDH expression (E3-KI: 0.0033±0.00044; E4-KI: 0.0036±0.00062; $p = 0.68$), KCC2:GAPDH expression (E3-KI: 0.052±0.0046; E4-KI: 0.055±0.0063; $p = 0.74$), or NKCC1:KCC2 expression (E3-KI: 0.067±0.014; E4-KI: 0.066±0.0063; $p = 0.98$) (Fig. 1B) as measured on 4-12% Bis-Tris gradient gels. n = 5 for apoE3-KI and 8 for apoE4-KI.

At 18 MO, apoE4-KI mice had significantly higher NKCC1:GAPDH than apoE3-KI mice (E3-KI: 0.0012±0.000082; E4-KI: 0.0032±0.000042; p = 0.0028), as measured on a 12% Bis-Tris gel. KCC2:GAPDH expression did not differ between apoE3- and apoE4-KI mice (E3-KI: 0.022±0.00069; E4-KI: 0.019±0.0014; p = 0.18), but the overall NKCC1:KCC2 ratio was elevated in apoE4- relative to apoE3-KI mice (E3-KI: 0.054±0.0049; E4-KI: 0.17±0.018; p = 0.00095). Together these results demonstrate that apoE4-KI mice have higher NKCC1:KCC2, driven by NKCC1, relative to apoE3-KI mice (Fig. 1C). n = 4 for apoE3-KI and 4 for apoE4-KI. This phenotype is age-dependent and emerges concurrently with, or after, cellular losses and learning and memory deficits (which develop between 12-16 MO). For consistency with previous results, NKCC1:GAPDH was also measured on a 4-12% gradient gel; these results confirmed that NKCC1:GAPDH is elevated in apoE4-KI mice (E3-KI: 0.0014±0.000040; E4-KI: 0.0022±0.000044; p = 0.0028) (Fig. 1D). n = 2 for apoE3-KI and 2 for apoE4-KI.

To explore the contribution of hippocampal subregions to the elevated NKCC1:KCC2 phenotype in apoE4-KI mice, I used fluorescence immunohistochemistry to measure NKCC1 expression in the CA1, CA3, and hilus of the hippocampus in 18 MO apoE3- and apoE4-KI mice (n = 4 brains per genotype). MAP2 was used as a neuronal stain, but was not used for quantification. NKCC1 expression was significantly higher in apoE4- relative to apoE3-KI mice in the hilus (E3-KI: 30.85±0.53; E4-KI: 32.96±0.78; p = 0.025) (Fig. 2A,D) and CA1 (E3-KI: 30.35±0.64; E4-KI: 32.47±0.60; p = 0.021) (Fig. 2B,D); expression also trended higher in CA3 but was not significant (E3-KI: 36.40±0.80; E4-KI: 38.57±0.93; p = 0.084) (Fig. 2C,D). By contrast, KCC2 expression did not differ in the CA1 (E3-KI: 30.54±0.50; E4-KI: 30.21±0.68; p = 0.71) (Fig. 4F,H) or CA3 (E3-KI: 30.37±0.69; E4-KI: 29.33±0.68; p = 0.29)(Fig. 4G,H); in the hilus, KCC2

expression trended higher in apoE3- over apoE4-KI mice at 18MO, but did not reach significance (E3-KI: 31.37±0.62; E4-KI: 29.74±0.62; p = 0.072)(Fig. 4E,H).

Chronic Bumetanide Treatment Rescues Memory in Aged ApoE4-KI Mice

Given the age- and genotype-dependent elevation of NKCC1:KCC2 in apoE4-KI mice, we assessed the NKCC1 inhibitor bumetanide as a therapeutic strategy via chronic systemic administration in mice aged to 16 MO, an age at which learning and memory deficits have been observed in apoE4-KI mice. The experimental timeline is shown in Fig. 3A.

ApoE3-KI and apoE4-KI mice were randomly assigned to Vehicle (2% DMSO in 0.9% Saline, pH 8.5), Low Bumetanide (0.02mg/kg Bumetanide in 2% DMSO and 0.9% Saline, pH 8.5) or High Bumetanide (0.2mg/kg Bumetanide in 2% DMSO and 0.9% Saline, pH 8.5) groups. At the start of treatment, n=10 apoE3-KI mice were assigned to Vehicle (age 14.01±0.44), n=11 apoE3-KI mice were assigned to Low Bumetanide (age 14.30±0.33), n = 10 apoE3-KI mice were assigned to High Bumetanide (age 13.74±0.22), n=10 apoE4-KI mice were assigned to Vehicle (age 14.10±0.35), n=10 apoE4-KI mice were assigned to Low Bumetanide (age 14.70±0.27), and n=9 apoE4-KI mice were assigned to High Bumetanide (age 13.77±0.28). Treatment was administered daily by i.p. injection for 62 days prior to the start of Morris Water Maze, and continued throughout the 14-day testing period. Age at Morris Water Maze assessment for E3/Vehicle, E3/Low Bumetanide, E3/High Bumetanide, E4/Vehicle, E4/Low Bumetanide, and E4/High Bumetanide were 16.06, 16.34, 15.78, 16.14, 16.74, and 15.81 months, respectively. Treatment was continued for 35 additional days prior to the administration of Open Field and

Eleveated Plus Maze tests. Mice were killed by saline perfusion 4 hours after final injection, and 1 day after Open Field assessment.

Chronic systemic bumetanide treatment did not affect learning behavior in this cohort (Fig. 3B). However, bumetanide treatment did improve memory behavior as assessed by probe trials at 24 (Fig. 3C), 72 (Fig. 3D), and 120 (Fig. 3E) hours after hidden training. At 24 hours (Fig. 3C), all groups showed a significant preference for the target quadrant except E4 Vehicle and E3 High Bumetanide; this suggests that bumetanide treatment rescues E4-releated memory deficits. Strikingly, by probe 2 and 3, *only* the E4 High Bumetanide group showed significant target quadrant preference, although there was a strong trend for E3 High Bumetanide mice ($p = 0.12$ and $p = 0.080$ at 72 and 120 hours, respectively). In open field test (Fig. 3F), there was no drug effect from bumetanide treatment, although there was a significant genotype effect ($p = 0.0074$). In elevated plus maze there was no bumetanide effect (Fig. 3G). Together these results suggest that bumetanide acts selectively on memory at 16 MO in E4-KI mice, but does not affect other behaviors.

Chronic Bumetanide Treatment Rescues Learning in Very Old ApoE4-KI Mice

Significant deficits in learning and memory can be observed in apoE4-KI mice by 16 MO. However, few studies have examined these mice at very old age (>20 MO). We assessed the effect of the High Bumetanide treatment (0.2 mg/kg) used in the 18 MO cohort on mice at the advanced age of 24 MO. The experimental timeline is shown in Fig. 4A.

ApoE3- and apoE4-KI mice were randomly assigned to Vehicle (2% DMSO in 0.9% Saline, pH 8.5) or Bumetanide (0.2mg/kg Bumetanide in 2% DMSO and 0.9% Saline, pH 8.5) groups. At

the start of treatment, n=11 apoE3-Ki mice were assigned to Vehicle (age 23.04±0.26), n = 11 apoE3-Ki mice were assigned to Bumetanide (age 22.79±0.15), n=11 apoE4-Ki mice were assigned to Vehicle (age 21.93±0.75), and n=11 apoE4-Ki mice were assigned to Bumetanide (age 23.01±0.14). Treatment was administered daily by IP injection for 30 days prior to the start of Morris Water Maze, and continued throughout the 14-day testing period; this shorter injection time period was chosen due to concerns over longevity for mice at this age. Age at Morris Water Maze assessment for E3/Vehicle, E3/Bumetanide, E4/Vehicle, and E4/Bumetanide were 24.43, 24.18, 23.32, and 24.40 months, respectively.

In hidden learning trials (Fig. 4B), two-way ANOVA showed a significant effect ($p < 0.05$). Post-hoc tests revealed that E4/Vehicle mice had significantly longer escape latency than E3/Vehicle mice (i.e., worse learning performance) on hidden days 1 ($p = 0.0017$) and 2 ($p = 0.000030$), indicating a genotype-dependent effect on learning at this age. E4/Vehicle mice also had significantly longer escape latency than E4/Bumetanide mice on hidden days 1 ($p = 0.038$), 2 ($p = 0.0015$), and 3 ($p = 0.020$), indicating a significant drug effect on learning in aged E4-KI mice. E3/Bumetanide mice also had lower escape latency than E4/Vehicle mice on days 1 ($p = 0.0023$), 2 ($p = 0.00010$) and 3 ($p = 0.022$); although E3/Vehicle and E3/Bumetanide mice did not statistically separate, suggesting that there was no additional drug effect in apoE3-KI mice at this age. E4/Bumetanide mice also outperformed E3/Vehicle mice on hidden day 4 only ($p = 0.042$). There was no significant difference in escape latency in visible trials between any groups. Taken together these results suggest that apoE4-KI mice have impaired learning at 24 MO relative to apoE3-KI mice, and that bumetanide treatment improves learning in apoE4- but not apoE3-KI mice.

In probe trials conducted 24 (Fig. 4C), 72 (Fig. 4D), and 120 (Fig. 4E) hours after the final hidden learning trial, all genotype and treatment groups significantly preferred the target quadrant over the mean of the off-target quadrants by percent time spent. Therefore, no conclusions could be drawn regarding drug and genotype on memory at 24 MO.

Figure 1. Expression of NKCC1 and KCC2 in apoE3- and apoE4-KI mice at 2, 10, and 18 MO

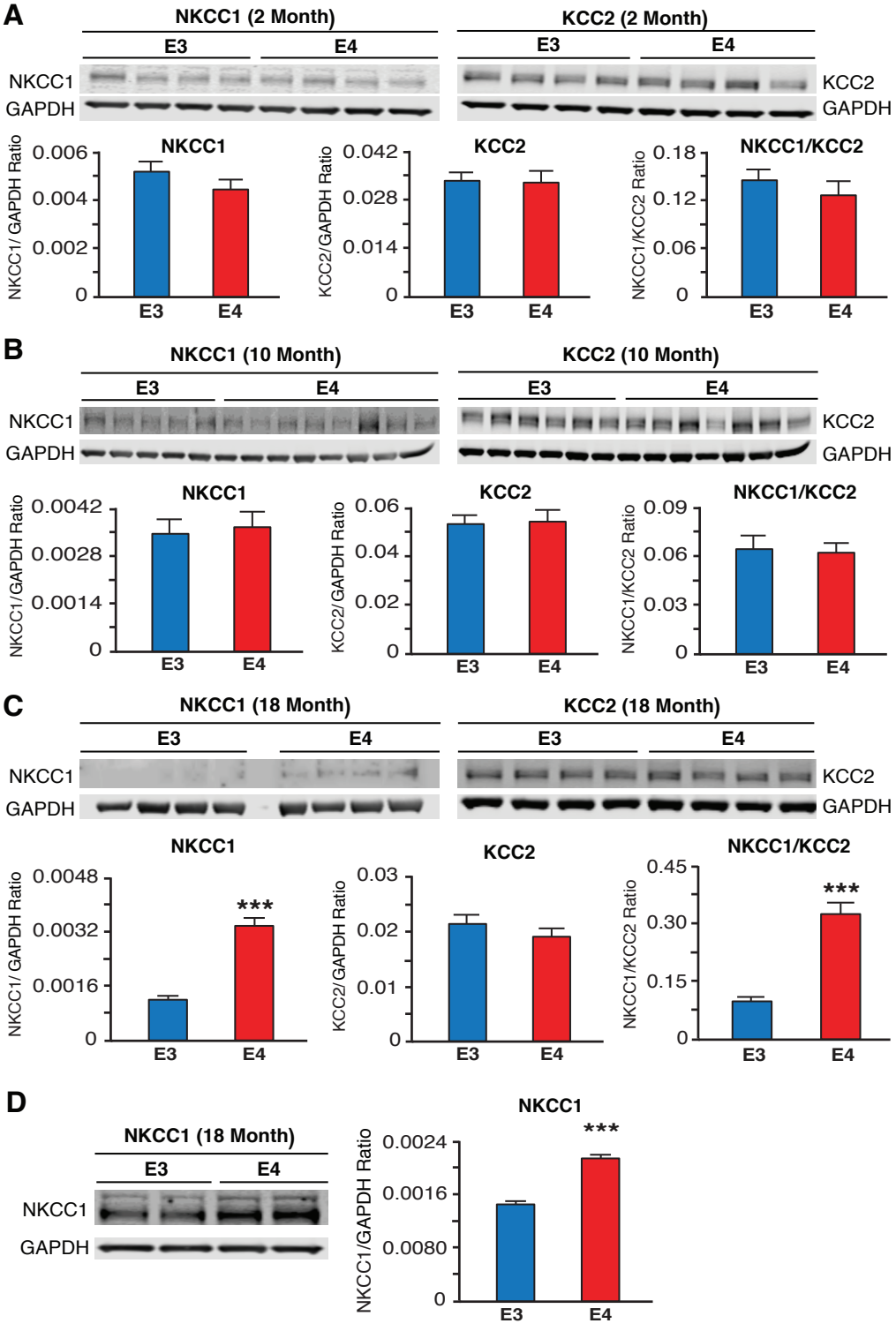

(A) Blot images, and quantification, of hippocampal samples from 2 MO apoE3- and apoE4-KI female mice blotted for NKCC1, KCC2, and GAPDH on 4-12% gradient gels. 2 MO mice did not differ in NKCC1, KCC2, or NKCC1:KCC2 ratio. n = 4, each genotype. **(B)** Blot images, and quantification, of hippocampal samples from 10 MO apoE3- and apoE4-KI female mice blotted for NKCC1, KCC2, and GAPDH on 4-12% gradient gels. 10 MO mice did not differ in NKCC1, KCC2, or NKCC1:KCC2 ratio. n = 5 apoE3-KI, 8 apoE4-KI. **(C)** Blot images, and quantification, of hippocampal samples from 18 MO apoE3- and apoE4-KI female mice blotted for NKCC1, KCC2, and GAPDH on 12% gels. 18 MO apoE4-KI mice had significantly higher NKCC1 and NKCC1:KCC2 ratio than apoE3-KI mice. n = 4, each genotype. **(D)** Blot images, and quantification, of hippocampal samples from 18 MO apoE3- and apoE4-KI female mice blotted for NKCC1 and GAPDH on 4-12% gradient gels. ApoE4-KI mice had significantly higher NKCC1 than apoE3-KI mice. n = 2, each genotype.

Figure 2. Immunofluorescent analysis of NKCC1 and KCC2 expression in the hippocampus of 18-month-old apoE3- and apoE4-KI mice

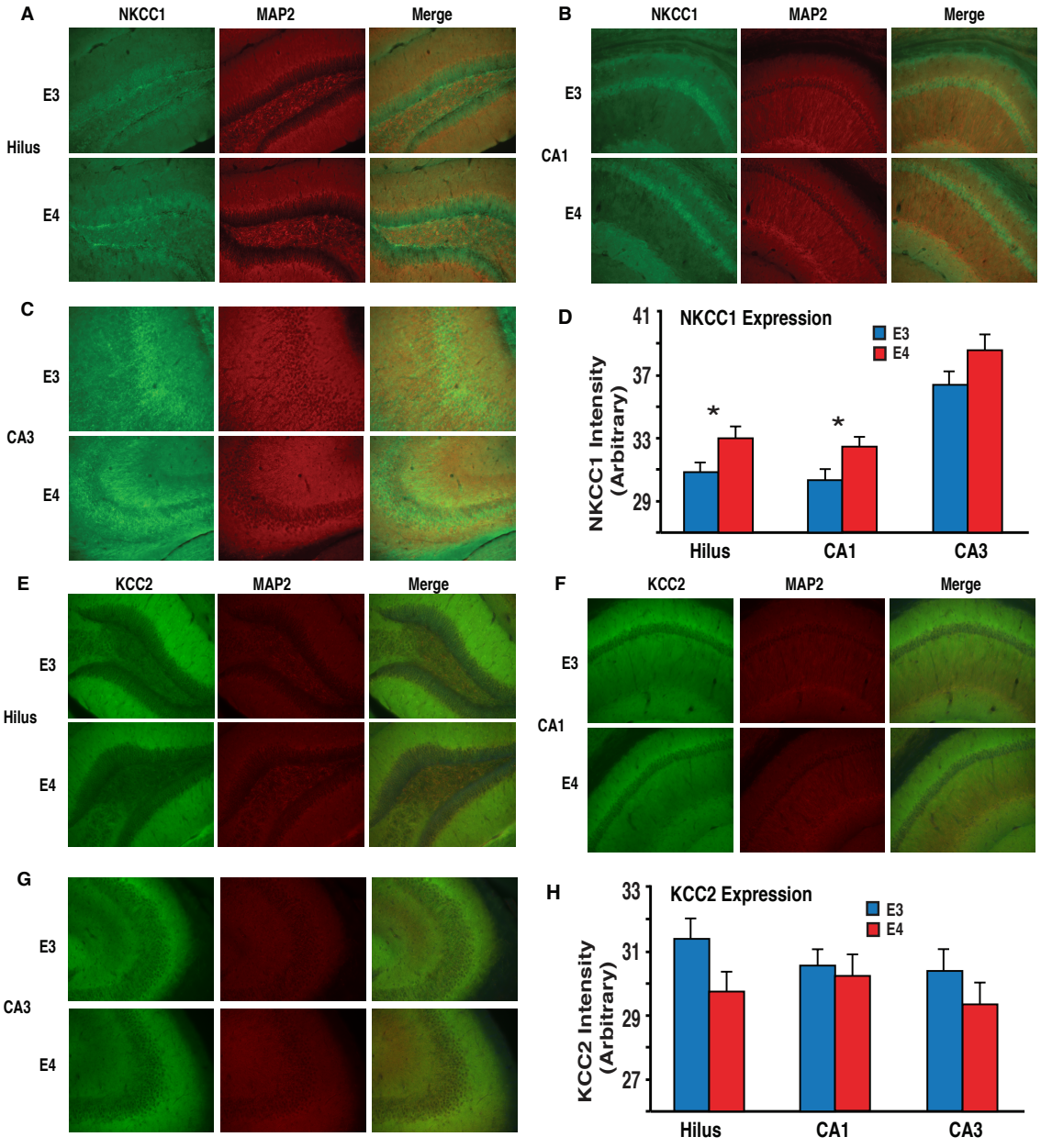

(A) Representative images of hilus from 18 MO apoE3- and apoE4-KI female mice, stained for NKCC1 and MAP2. **(B)** Representative images of CA1 from 18 MO apoE3- and apoE4-KI female mice, stained for NKCC1 and MAP2. **(C)** Representative images of CA3 from 18 MO apoE3- and apoE4-KI female mice, stained for NKCC1 and MAP2. **(D)** Quantification of n = 4 mice per group

from images as in **(A,B,C)**. NKCC1 was significantly higher in apoE4-KI mice in the hilus and CA1. **(E)** Representative images of hilus from 18 MO apoE3- and apoE4-KI female mice, stained for KCC2 and MAP2. **(F)** Representative images of CA1 from 18 MO apoE3- and apoE4-KI female mice, stained for KCC2 and MAP2. **(C)** Representative images of CA3 from 18 MO apoE3- and apoE4-KI female mice, stained for KCC2 and MAP2. **(G)** Quantification of n = 4 mice per group from images as in **(E,F,G)**. There were no significant differences in KCC2 expression between apoE3- and apoE4-KI mice in any of the regions examined.

Figure 3. Effects of *in vivo* chronic bumetanide treatment on aged apoE3- and apoE4-KI mice

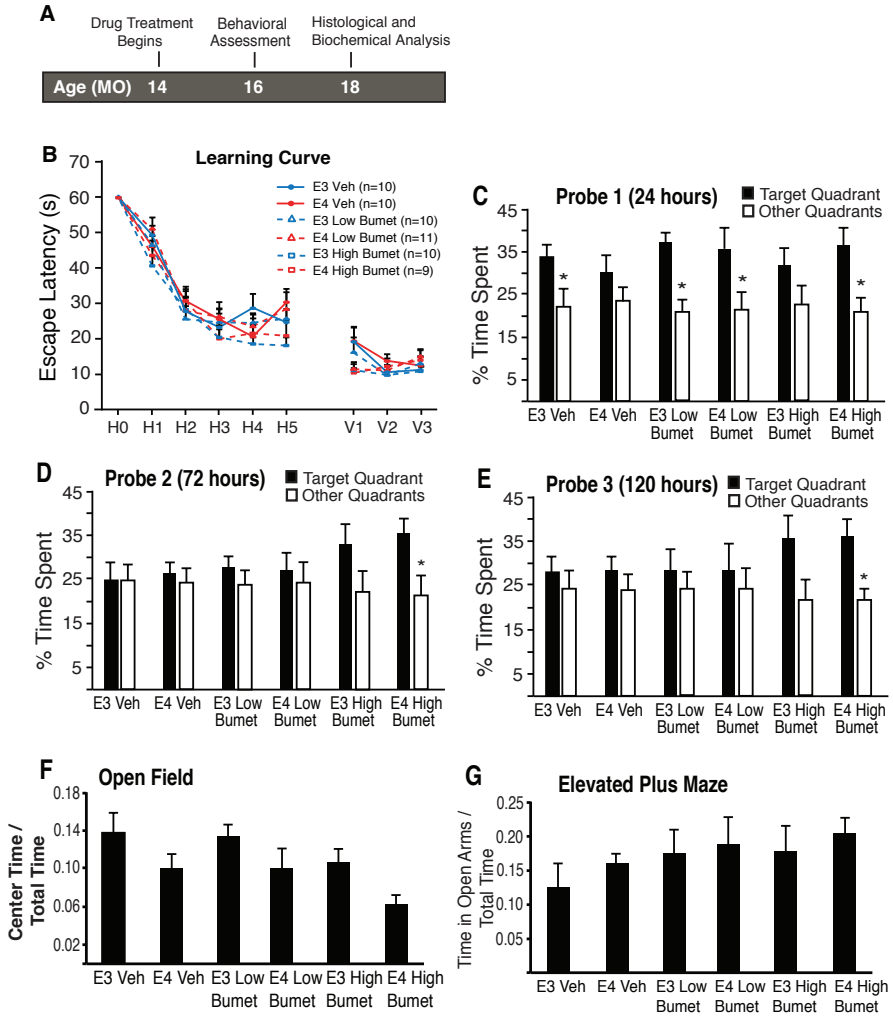

(A) Experimental timeline for mouse cohort with age shown in months old (MO). **(B)** Morris water maze (MWM) showed no difference in escape latency between genotype and treatment groups. Points represent averages of daily trials. H, hidden platform day (two trials/session, two sessions/day); H0, first trial on H1; V, visible platform day (three trials / session, one session). Y axis indicates time to reach the target platform. **(C-E)** bumetanide treatment rescued memory in apoE4-KI mice at 24, 72, and 120 hours after hidden trials. **(F-G)** There was no significant difference by treatment in Elevated Plus Maze and Open Field Maze tests.

Figure 4. Effects of *in vivo* chronic bumetanide treatment on very old apoE3- and apoE4-KI mice

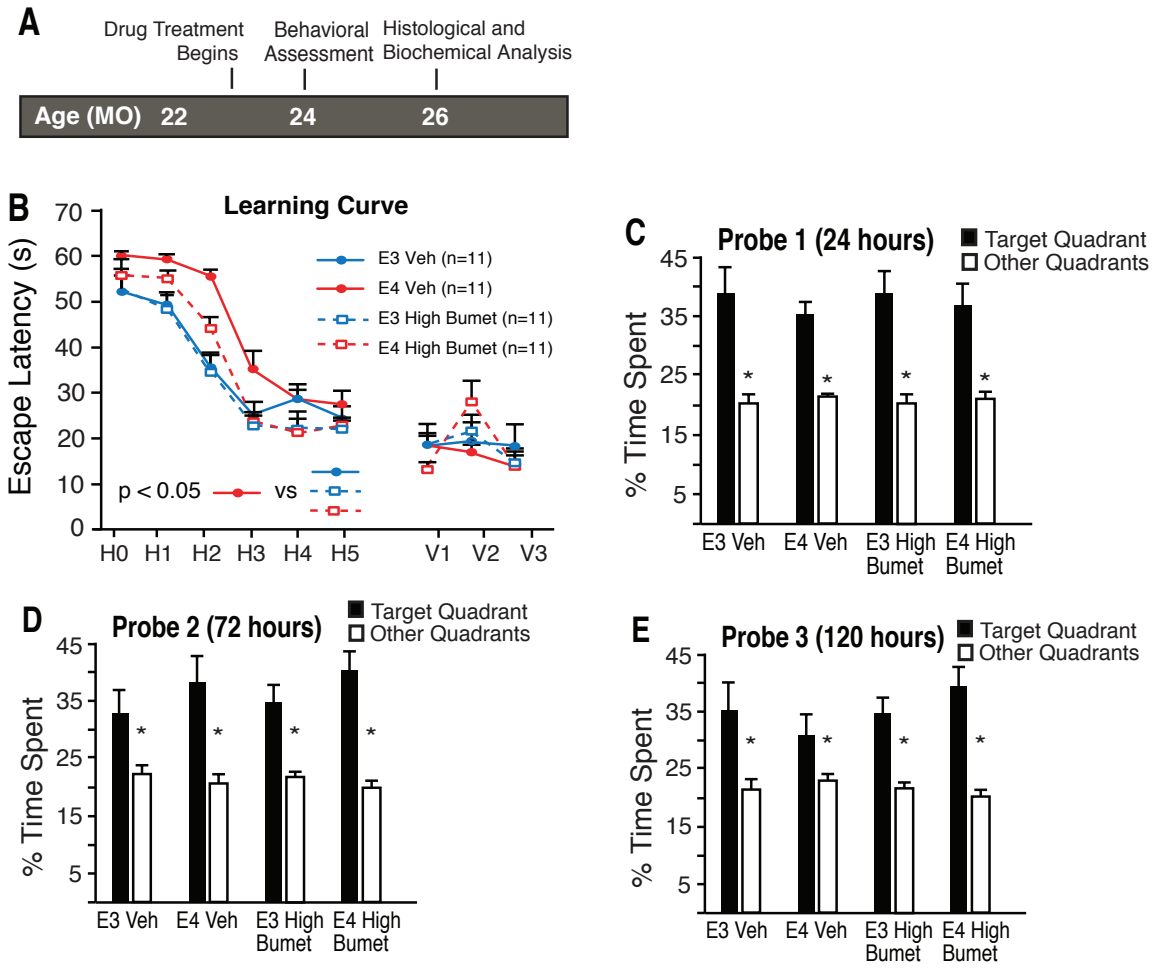

(A) Experimental timeline for mouse cohort with age shown in months old (MO). **(B)** Morris water maze (MWM) showed significantly longer escape latency for apoE4-KI vehicle mice. Points represent averages of daily trials. HD, hidden platform day (two trials/session, two sessions/day); H0, first trial on H1; V, visible platform day (three trials / session, one session). Y axis indicates time to reach the target platform. **(C-E)** All groups showed significant preference for target quadrant at 24, 72, and 120 hours after hidden trials.

Chronic Bumetanide Treatment Normalizes NKCC1:KCC2 in Aged ApoE4-KI Mice

Bumetanide is well-established as an inhibitor of NKCC1 activity. However, in the pursuit of a disease-modifying treatment for AD, we investigated whether bumetanide also alters the NKCC1:KCC2 ratio in apoE4-KI mice.

Samples were collected from the mouse cohort in Fig. 3A and prepared for Western Blotting as described (see Methods). Samples from 18 MO apoE4-KI mice treated chronically with 0.2mg/kg bumetanide or saline vehicle daily for 4 months were compared. 18 MO bumetanide-treated apoE4-KI mice did not differ from vehicle-treated apoE4-KI mice in NKCC1 (E4-KI Vehicle: 0.0067±0.00021; E4-KI Bumetanide: 0.0060±0.00072; p = 0.35) (Fig. 5A,C) or KCC2 (E4-KI Vehicle: 0.040±0.0037; E4-KI Bumetanide: 0.071±0.017; p = 0.071) (Fig. 5B,D) expression individually. However, bumetanide-treated apoE4-KI mice had significantly lower overall NKCC1:KCC2 ratio than vehicle-treated apoE4-KI mice (E4-KI Vehicle: 0.17±0.019; E4-KI Bumetanide: 0.091±0.013; p = 0.011) (Fig. 5E). n = 4 for vehicle and 4 for bumetanide. Strikingly, a larger contribution to the ratio normalization comes from KCC2 than NKCC1; in early development, both NKCC1 and E_{Cl} are thought to regulate KCC2 expression, suggesting a mechanism for this effect.

Deletion of ApoE4 in Forebrain Interneurons Normalizes CCC Expression

Previous work from our lab examined the contribution of apoE4 produced by various cell types to cognitive and cellular deficits in aged apoE-KI mice. Deletion of apoE4 in neurons was sufficient to rescue apoE4-driven deficits; indeed, deletion of apoE4 in forebrain *interneurons* only was also sufficient (Knoferle et al., 2014). This deletion was achieved developmentally by

crossing a LoxP floxed apoE-KI line with a line expressing Cre under the control of a forebrain interneuron enhancer, Dlx; the resulting line is known as Dlx/E4-KI, and is cognitively normal with respect to apoE3-KI mice (Knoferle et al., 2014).

Since the Dlx/E4-KI line does not have the cognitive deficits seen in apoE4-KI mice, we examined whether deletion of apoE4 in forebrain interneurons also alters CCC expression. Hippocampal tissue was harvested and prepared for Western Blotting (see Methods) from female Dlx/E4-KI mice, aged 18 MO (Fig. 6A).

18 MO Dlx/E4-KI mice had significantly lower NKCC1 expression than apoE4-KI mice (Dlx/E4-KI: 0.0086±0.00034; E4-KI: 0.0059±0.00091; $p = 0.035$) (Fig. 6B), but did not significantly differ in KCC2 expression (Dlx/E4-KI: 0.024±0.0012; E4-KI: 0.031±0.0051; $p = 0.22$) (Fig. 6B). The overall ratio of NKCC1:KCC2 expression in Dlx/E4-KI mice was also lower than in apoE4-KI mice at this age (Dlx/E4-KI: 0.36±0.019; E4-KI: 0.19±0.016; $p = 0.0056$) (Fig. 6B). n = 4 for apoE4-KI and 4 for Dlx/E4-KI.

To assess whether this rescue was partial or complete, 18 MO apoE3-KI, apoE4-KI, and Dlx/E4-KI tissue was assessed on the same gel (Fig. 6C). 18 MO Dlx/E4-KI more closely resembled apoE3-KI than apoE4-KI mice in terms of NKCC1:GAPDH expression (E4-KI: 0.0047±0.000332; Dlx/E4-KI: 0.0037±0.00081; E3-KI: 0.0036±0.00050), KCC2:GAPDH expression (E4-KI: 0.036±0.0024; Dlx/E4-KI: 0.043±0.0085; E3-KI: 0.039±0.0036), and NKCC1:KCC2 expression (E4-KI: 0.14±0.018; Dlx/E4-KI: 0.086±0.017; E3-KI: 0.092±0.0060) (Fig. 6D). While strong trends were observed in the NKCC1:KCC2 ratio difference between apoE3-KI vs. apoE4-KI mice ($p = 0.086$) and Dlx/E4-KI vs. apoE4-KI mice ($p = 0.11$), no differences reached statistical significance due to low n in this study (n = 3 per genotype) (Fig. 6D).

Short-term Pentobarbital Treatment Does Not Affect CCC Expression

A previous study from our lab showed that treating apoE4-KI mice at 16 MO with the $GABA_AR$ potentiator pentobarbital for two weeks at 20mg/kg; this dose rescued learning and memory behavior in MWM but did not restore interneuron numbers (Tong et al., 2016). To assess whether acutely increasing inhibition would affect CCC expression, apoE4-KI mice were treated for 14 days with 20mg/kg pentobarbital or equivalent volume of sterile saline. At the time of tissue collection, mice were 17 MO.

Short-term pentobarbital treatment did not significantly affect expression of NKCC1:GAPDH (E4-KI/Vehicle: 0.0053±0.0012; E4-KI/Pentobarbital: 0.0070±0.00060; p = 0.25) (Fig. 7A,C). Expression of KCC2:GAPDH was unchanged in vehicle-treated vs. pentobarbital-treated apoE4-KI mice (E4-KI/Vehicle: 0.018±0.0035; E4-KI/Pentobarbital: 0.018±0.0013; p = 0.92) (Fig. 7B,D). Overall ratio of NKCC1:KCC2 in vehicle-treated vs. pentobarbital-treated mice was not statistically significant, but pentobarbital treatment trended toward a higher ratio (E4-KI/Vehicle: 0.30±0.032; E4-KI/Pentobarbital: 0.40±0.049; p = 0.13) (Fig. 7E). n = 4 for vehicle and 4 for pentobarbital. Therefore, we concluded that pentobarbital treatment, in the context of interneuron losses in aged apoE4-KI mice, did not normalize NKCC1:KCC2 expression.

Figure 5. Chronic Bumetanide Treatment Reduces NKCC1:KCC2 Ratio in Aged ApoE4-KI Mice

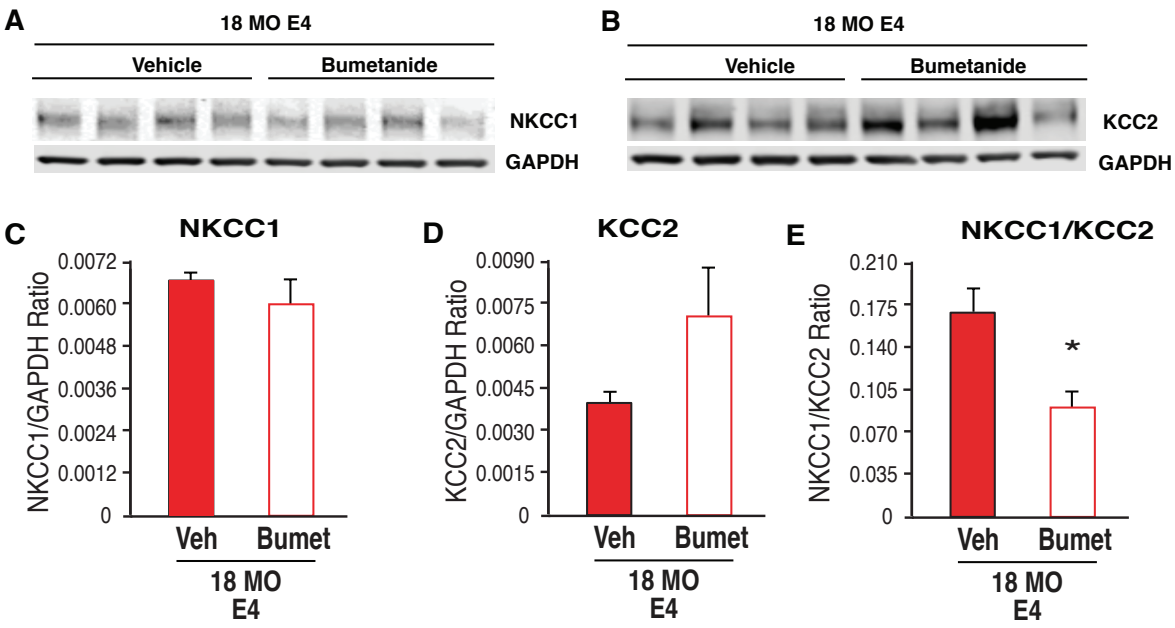

(A) Representative Western Blot of NKCC1 expression (with GAPDH loading control) in vehicle- and bumetanide-treated 18 MO ApoE4-KI mice. **(B**) Representative Western Blot of KCC2 expression (with GAPDH loading control) in vehicle- and bumetanide-treated 18 MO ApoE4-KI mice. **(C)** Quantification of (A). Bumetanide treatment did not significantly change NKCC1 expression. **(D)** Quantification of (B). Bumetanide-treated mice strongly trended toward higher KCC2 expression. **(E)** Quantification of (A) and (B). Bumetanide-treated apoE4-KI mice had significantly lower overall NKCC1:KCC2 ratio than vehicle-treated mice. n = 4, each group.

Figure 6. Effects of Deleting ApoE in Forebrain Interneurons on CCC Expression in Aged ApoE4-KI Mice

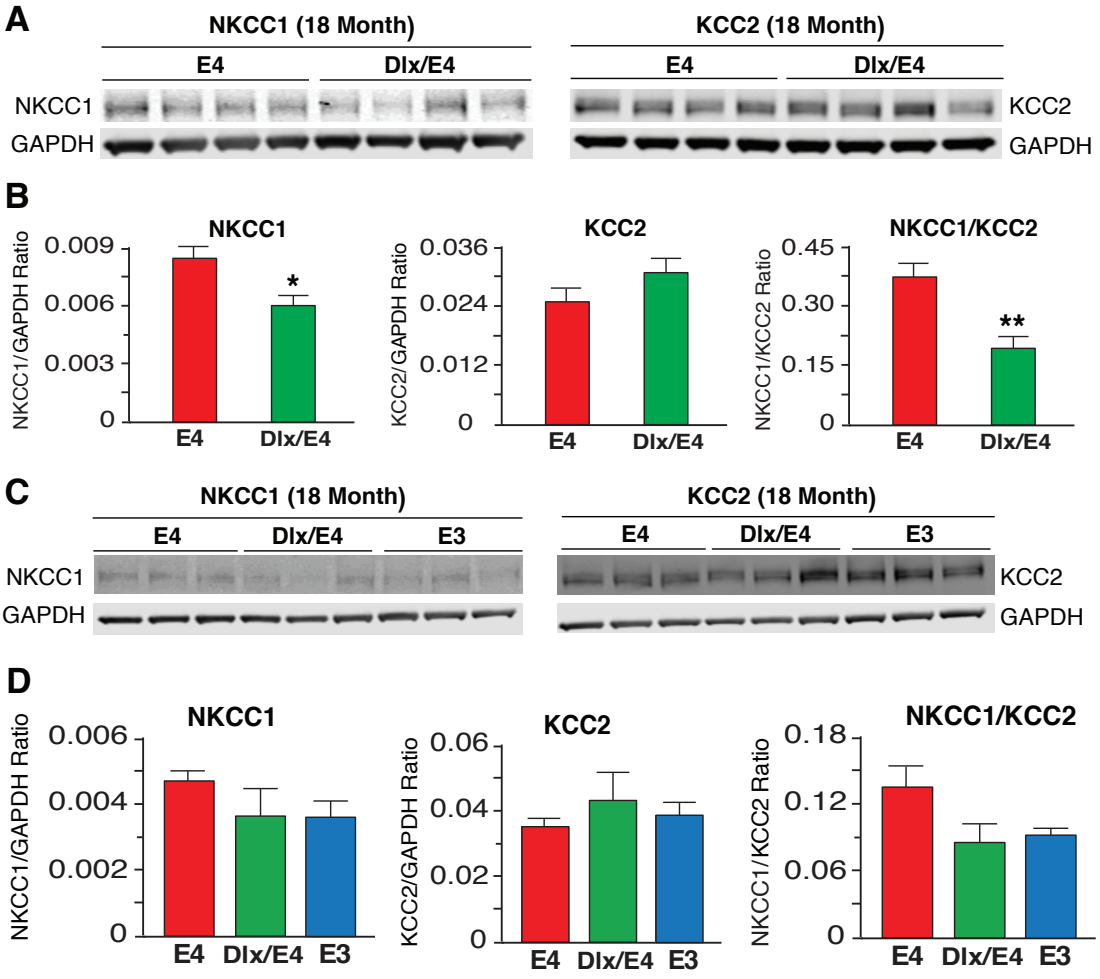

(A) Representative Western Blot of NKCC1 and KCC2 expression (with GAPDH loading control) in vehicle- and bumetanide-treated 18 MO apoE4-KI and Dlx-Cre/E4-fKI mice on 4-12% gradient gels. **(B)** Quantification of (A). Dlx/E4 mice had lower NKCC1, trended toward higher KCC2, and had lower overall NKCC1:KCC2 ratio. n = 4, each group. **(C)** Representative Western Blot of NKCC1 and KCC2 expression (with GAPDH loading control) in vehicle- and bumetanide-treated 18 MO apoE4-KI and Dlx-Cre/E4-fKI mice on 4-12% gradient gels. **(D)** Quantification of (C). n = 3, each group.

Figure 7. Effects of Short-term Pentobarbital Treatment on CCC Expression in Aged ApoE4-KI Mice

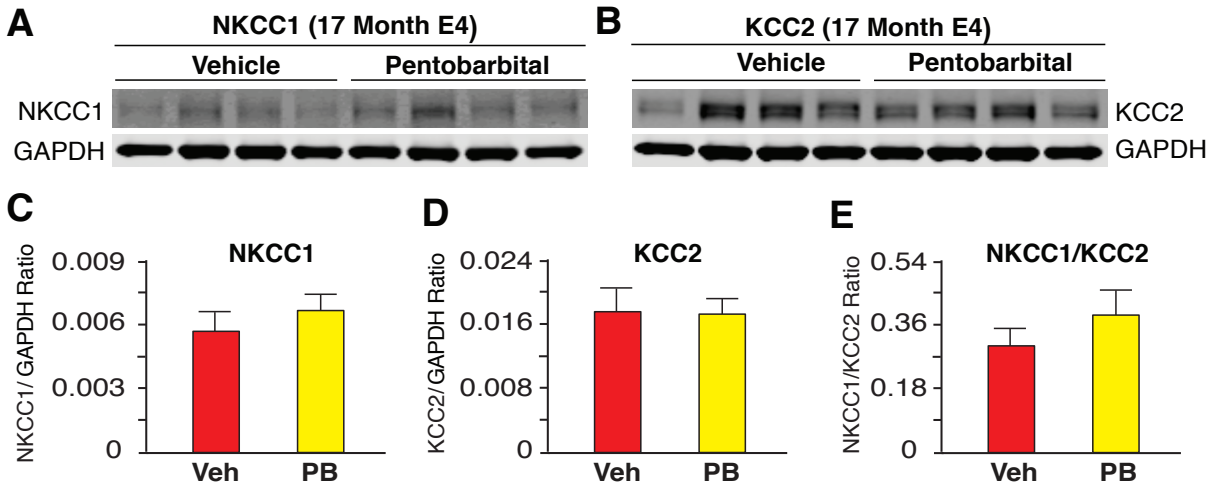

(A) Representative Western Blot of NKCC1 expression (with GAPDH loading control) in vehicle- and pentobarbital-treated 17 MO ApoE4-KI mice. **(B**) Representative Western Blot of KCC2 expression (with GAPDH loading control) in vehicle- and pentobarbital-treated 17 MO ApoE4-KI mice. **(C)** Quantification of (A). Pentobarbital treatment had no effect on NKCC1 expression. **(D)** Quantification of (B). Pentobarbital treatment had no effect on KCC2 expression. **(E)** Quantification of (A) and (B). Pentobarbital had no effect on NKCC1:KCC2 ratio. n = 4, each group.

CHAPTER 4

GABA Receptor δ Overexpression Restores Learning and Memory and Rescues Interneuron Numbers in ApoE4 Knock in Mice

Viral Overexpression of $GABA_AR$ Subunit δ

In order to study the *in vivo* effects of overexpression $GABA_AR$ subunit δ in apoE-KI mice, apoE3- and apoE4-KI mice were aged to 16 MO and randomly assigned to receive stereotaxic injections of lentivirus carrying GFP only or GFP/δ directly into the hilus of the dentate gyrus. Experimental timeline is shown in Fig. 8A.

At injection, n = 10 apoE3-KI mice were assigned to GFP/δ (age 16.57±0.13), n = 13 apoE3-KI mice were assigned to GFP (age 16.36±0.16), n = 9 apoE4-KI mice were assigned to GFP/δ (age 16.76±0.17), and n = 11 apoE4-KI mice were assigned to GFP (age 16.59±0.34); there were no significant age differences between genotype or virus groups. Viral injections were completed over a one-week period.

Beginning at 5 weeks post-injection and continuing to 14 weeks post-injection, mice were subjected to a battery of behavioral tests to assess movement, anxiety, learning, memory, and cognitive flexibility (see below). At 18 weeks post-injection, mice were perfused and floating brain section immunohistochemistry was performed to assess expression of target proteins. Immunohistochemistry for GFP and δ showed that expression of GFP or GFP and δ was robust in the hilus of the dentate gyrus (Fig. 8B); coexpression of GFP and δ was significantly higher in mice injected with GFP/δ construct as measured by colocalization between the red (δ) and green (GFP) channels (GFP: 0.35±0.11; GFP-δ: 0.83±0.046 Pearson's R;

p = 0.00025) (Fig. 8C). Scrambled control images had a coherence below the limit of detection, indicating that this effect was not an artifact (Scrambled: 0.00±0.00 Pearson's R; p = 0.00). n = 17 δ/GFP and 17 GFP.

Overexpression of $GABA_AR$ Subunit δ Improves Stamina, But Does Not Affect Exploratory Behavior, in Aged ApoE-KI Mice

5 weeks following viral injections, movement behavior was assessed in Open Field Maze and Rotarod tests.

In the Rotarod test, δ overexpression improved stamina over control (GFP only) in apoE4- (E4-GFP: 201.09±11.67 s; E4-δ: 240.44±10.19; p = 0.033) but not apoE3-KI (E3-GFP: 154.72±15.65 s; E3-δ: 166.62±15.41; p = 0.48) mice (Fig. 9A). Control apoE3-KI mice had significantly less endurance than both control apoE4-KI mice and δ overexpressing apoE4-KI mice (p = 0.030 E3-GFP vs. E4-GFP; p = 0.0005 E3-GFP vs. E4-δ), while δ overexpressing apoE3-KI mice had significantly less endurance than δ overexpressing apoE4-KI mice (p = 0.0014 E3-δ vs. E4-δ) but only trended toward lower endurance than control apoE4-KI mice (p = 0.093 E3-δ vs. E4-GFP). Overall, apoE4-KI mice significantly outperformed apoE3-KI mice (E3-KI: 160.17±10.86 s; E4-KI: 217.96±8.92 s; p = 0.00022) (Fig. 9B). Since weight gain is an established feature of apoE3-KI mice, we examined the relationship between weight and Rotarod performance in this cohort. Overall, apoE3-KI mice weighed significantly more during Rotarod assessment than apoE4-KI mice (E3-KI: 32.31±1.41 g; E4-KI: 26.20±0.82 g; p = 0.00078), but there was no effect of δ overexpression on weight in either apoE3-KI mice (E3-GFP: 34.29±2.40 g; E3-δ: 29.96±0.84 g; p = 0.13) or apoE4-KI mice (E4-GFP: 26.23±1.35; E4-δ: 26.16±0.78; p =

0.96). Linear regression showed a highly significant correlation between mouse weight and Rotarod endurance (R^2 = 0.44; p = 7.7 x 10^{-7}) (Fig. 9C). When we built separate linear models for the two genotypes, weight significantly predicted rotarod performance in apoE3-KI mice (R^2 = 0.38; p = 0.0013); in apoE4-KI mice the correlation was trending but not significant (R^2 = 0.16; p = 0.074) (Fig. 9D).

In the Open Field Maze, there was no significant effect of δ overexpression within apoE3- (E3-GFP: 0.094±0.017; E3-δ: 0.099±0.022; p = 0.85) or apoE4-KI (E4-GFP: 0.063±0.014; E4-δ: 0.057±0.013; p = 0.76) mice (Fig. 9E). Overall, apoE4-KI mice a significantly higher proportion of time in the center of the maze than apoE3-KI mice (E3-KI: 0.096±0.013; E4-KI: 0.061±0.0094; p = 0.040).

Overexpression of $GABA_AR$ Subunit δ Normalizes Anxiety Behavior in Aged ApoE4-KI Mice

To assess the effect of δ overexpression on anxiety behavior in aged apoE-KI mice, mice were assessed in the Elevated Plus Maze 5 weeks after viral injection. Within the control (GFP-only) mice, apoE4-KI mice strongly trended toward less time in the closed maze arms than apoE3-KI mice (E3-GFP: 483.55±10.98 s; E4-GFP: 433.13±24.16 s; p = 0.063) (Fig. 10). This difference was ameliorated by δ overexpression in apoE4-KI mice and restored to apoE3-KI levels (E4-δ: 505.17±11.87 s; p = 0.026 vs. E4-GFP; p = 0.20 vs. E3-GFP) (Fig. 10). Overexpression of δ had no effect within apoE3-KI mice (E3-δ: 476.42±19.15; p = 0.75 vs. E3-GFP) (Fig. 10).

Overexpression of $GABA_AR$ Subunit δ Improves Cognitive Flexibility in Aged ApoE4-KI Mice

In order to assess the effect of δ overexpression on learning behavior in aged apoE-KI mice, mice were subjected to MWM. No significant differences were observed by treatment or genotype (Fig. 11A). In addition, no groups were able to find the platform with a mean latency below 25s, even after 6 days of hidden training. This poor asymptotic learning, in addition to the lack of difference between control apoE3- and apoE4-KI mice, suggested that the mice failed to understand the task.

At 24 hours after the final hidden trial, all groups showed significant preference for the target quadrant over the mean of the three off-target quadrants (E3-δ: 39.07±4.00 target vs. 20.44±1.33 off, p = 0.00033; E3-GFP: 34.01±4.10 target vs. 22.12±1.37 off, p = 0.011; E4-δ: 40.18±5.20 target vs. 19.89±1.54, p = 0.0013; E4-GFP: 36.93±3.89 target vs. 21.15±1.30 off, p = 0.0010) (Fig. 11B). At 72 hours after the final hidden trial, all groups continued to show significant preference for the target quadrant over the mean of the three off-target quadrants (E3-δ: 33.28±4.09 target vs. 22.36±1.36 off, p = 0.021; E3-GFP: 32.73±3.03 target vs. 22.55±1.010 off, p = 0.0040; E4-δ: 39.33±6.06 target vs. 20.34±2.019, p = 0.0090; E4-GFP: 34.18±4.30 target vs. 22.060±1.43 off, p = 0.015) (Fig. 11C).

Due to inconclusive results in the first MWM test, the mice were re-assessed in reversal MWM 6 weeks after the initial MWM. In reversal MWM, mice are first trained to locate the hidden platform (as in a standard MWM) over three days of training. Then, the platform is moved to the opposite quadrant (in this case, from the NE quadrant to the SW), and mice are re-trained to find this new platform location over an additional 5 days of hidden training. Since mice must forget the initial platform location and adapt to a new one, reversal MWM is considered a test of cognitive flexibility.

In reversal MWM, there were no significant differences in latency over the initial three-day training period ($p = 0.086$, two-factor ANOVA) (Fig. 11D). However, over the reversal days, two-factor ANOVA showed a significant learning difference ($p = 0.047$), with post-hoc tests revealing that the E4-GFP group performed significantly worse than all other groups overall ($p = 7.5 \times 10^{-9}$ vs. E3-δ; $p = 2.8 \times 10^{-8}$ vs. E3-GFP; $p = 4.7 \times 10^{-5}$ vs. E4-δ). The E4-GFP group performed significantly worse than all other groups on Reversal Day 4 ($p = 0.039$ vs. E3-δ; $p = 0046$ vs. E3-GFP; $p = 0.0065$ vs. E4-δ). E4-GFP mice performed worse than E3-δ mice on Reversal Day 5 ($p = 0.0078$) and trended strongly toward worse performance than E4-δ mice ($p = 0.053$). Taken together, these results suggest that apoE3-KI mice have greater cognitive flexibility than apoE4-KI mice at 19 MO, that δ overexpression rescues cognitive flexibility in aged apoE4-KI mice, and that δ overexpression has no additional effect on aged apoE3-KI mice.

Before progressing to the reversal trials, preference for the initial target quadrant was assessed in a probe trial 24 hours after the second hidden day. All groups showed significant preference for the target quadrant over the off-target quadrants as measured by percent of time spent in on-target vs. off-target quadrants (E3-GFP: 30.19±2.26 target vs. 20.63±0.71 off, $p = 0.00066$; E4-GFP: 37.78±3.16 target vs. 18.36±0.98 off, $p = 0.0000096$; E4-δ: 31.05±3.52 target vs. 21.07±1.34 off, $p = 0.018$) with the exception of the E3-δ group (23.18±2.91 target vs. 23.18±0.95 off, $p = 0.99$).

After the conclusion of reversal trials, preference for the new platform location was assessed in a second round of probe trials. At 24 hours after the final reversal trial, all groups showed a significant preference for the target quadrant by percent time spent (E3-GFP: 35.91±4.29 target vs. 18.94±1.47 off, $p = 0.0013$; E3-δ: 43.23±3.60 target vs. 16.62±1.13 off, $p =$

0.0000014; E4-GFP: 52.71±4.60 target vs. 12.97±1.56 off, p = 0.0.000000084; E4-δ: 52.12±3.39 target vs. 13.86±1.11 off, p = 0.000000010). At 72 hours after the final reversal trial, all groups continued to show a significant preference for the target location (E3-GFP: 37.87±3.97 target vs. 18.05±1.32 off, p = 0.00013; E3-δ: 43.18±3.40 target vs. 16.02±1.02 off, p = 0.00000046; E4-GFP: 54.76±2.43 target vs. 12.65±0.94 off, p = 6.1×10^{-13}; E4-δ: 51.29±3.85 target vs. 13.80±1.35 off, p = 0.000000088). Therefore, the effect of δ overexpression on memory could not be assessed in this cohort.

Overexpression of $GABA_AR$ Subunit δ Rescues Interneuron Numbers in Aged ApoE4-KI Mice

Given that δ overexpression is predicted to enhance tonic inhibition, and that excessive excitation is neurotoxic, we explored whether δ overexpression had a neuroprotective effect in this cohort. ApoE4-KI mice have an established deficit in somatostatin-positive interneurons in the dentate gyrus that is correlated to learning outcomes (Andrews-Zwilling et al., 2010). We used DAB staining (see Methods) to quantify somatostatin- (SOM) positive interneurons in apoE3- and apoE4-KI mice overexpressing either GFP and δ or GFP only (control) (Fig. 12A). Since every 10^{th} section was saved for floating section immunohistochemistry, the total number of SOM+ interneurons was extrapolated by multiplying the count by 10.

Consistent with previous studies, within the control treatment apoE3-KI mice had significantly more SOM+ interneurons than apoE4-KI mice (E3-GFP: 3202.63±232.49; E4-GFP: 2206.58±103.10; p = 0.00020) (Fig. 12B). δ overexpression significantly increased SOM+ interneuron count in apoE4-KI mice (E4-δ: 3206.945±246.36; p = 0.00060 vs. E4-GFP) and rescued the cell number to control apoE3-KI levels (p = 0.9903 vs. E3-GFP) (Fig. 12B). Within

apoE3-KI mice, δ overexpression also significantly increased SOM+ interneuron count over control (E3-δ: 3913.33±166.08; p = 0.0146 vs. E3-GFP) (Fig. 12B). This suggests that within both aged apoE3- and apoE4-KI mice, δ overexpression increases SOM+ interneurons in the dentate gyrus. Whether this observed effect is due to neuroprotection, neurogenesis, or increased expression of SOM is unknown.

Figure 8. Lentiviral Injection into Hippocampus Allowed Significant Overexpression of $GABA_AR$ Subunit δ in Aged ApoE-KI Mice

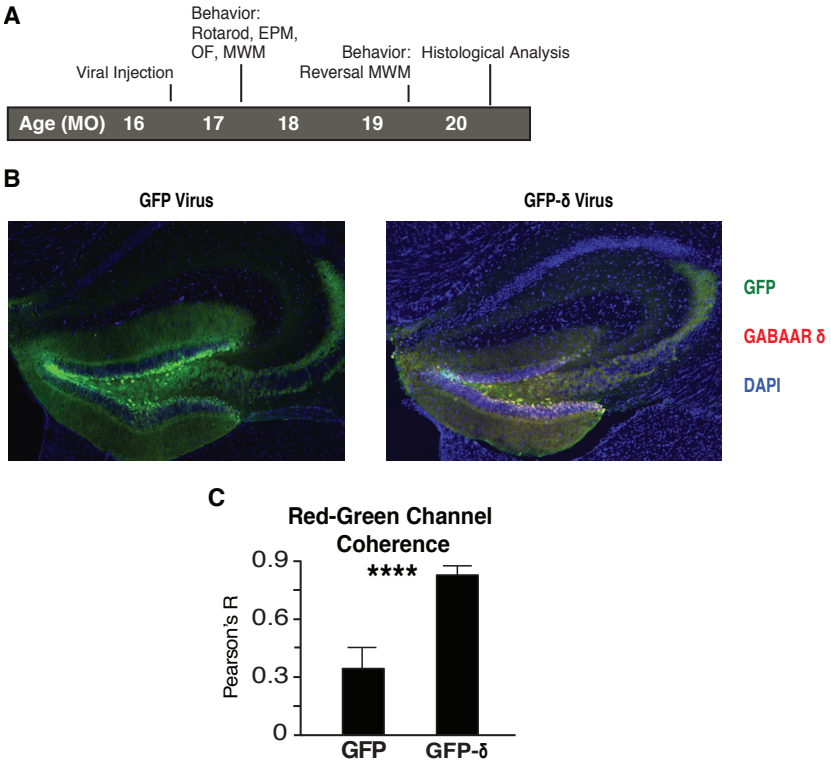

(A) Experimental timeline for mouse cohort, with age indicated in months old (MO). **(B)** Representatitive images from floating section immunohistochemistry experiment. Mice injected with lentivirus carrying GFP or GFP + δ, allowed to express protein for 4 months, then sectioned and stained for GFP (green) and δ (red) and mounted with DAPI (blue). **(C)** Colocalization analysis for red and green channels from images as shown in (B). There was significantly higher red-green colocalization in the GFP + δ group. n = 17 for both groups.

Figure 9. Hippocampal Overexpression of $GABA_AR$ Subunit δ Improves Stamina, But Does Not Affect Exploration, in Aged ApoE-KI Mice

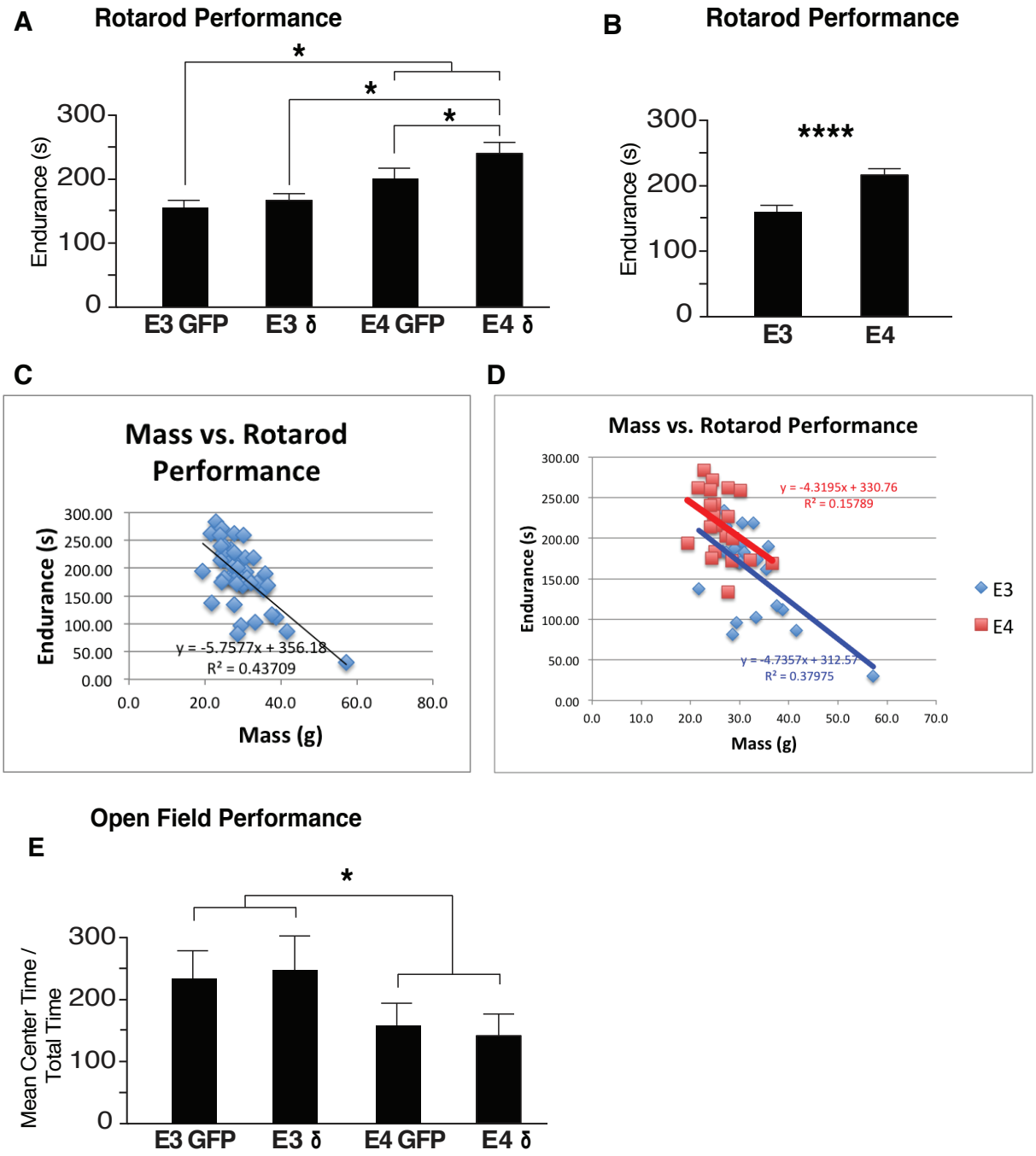

(A) Results of Rotarod test for 17MO apoE3- and apoE4-KI mice overexpressing GFP or GFP + δ in the dentate gyrus. δ overexpression improved endurance in apoE4-KI mice. **(B)** Results from (A), pooled by genotype. ApoE4-KI mice had significantly better endurance than apoE3-KI mice. **(C)** Linear regression on results from individual mice, showing correlation between weight (g)

and endurance (s). Weight was negatively correlated with endurance. **(D)** Data from (C), split by genotype. The correlation between weight and endurance was stronger in apoE3-KI mice. **(E)** Results of Open Field maze test for 17MO apoE3- and apoE4-KI mice overexpressing GFP or GFP + δ in the dentate gyrus. ApoE4-KI mice spent less time in the maze center than apoE3-KI mice, with no effect from δ.

Figure 10. Hippocampal Overexpression of $GABA_AR$ Subunit δ Normalizes Anxiety Behavior in Aged ApoE4-KI Mice

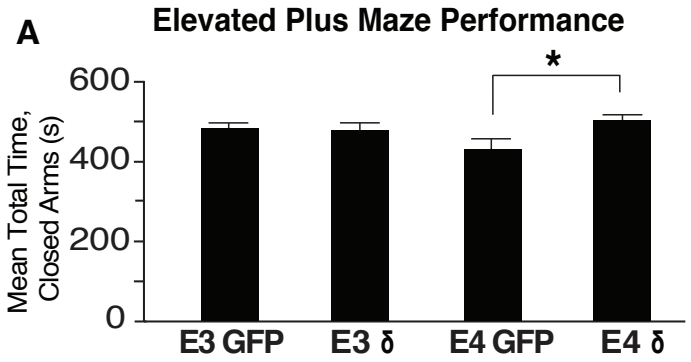

(A) Results of Elevated Plus Maze for 17MO apoE3- and apoE4-KI mice overexpressing GFP or GFP + δ in the dentate gyrus. δ overexpression restored time spent in closed arms in apoE4-KI mice to apoE3-like levels, but did not have any effect in apoE3-KI mice.

Figure 11. Hippocampal Overexpression of $GABA_AR$ Subunit δ Rescues Cognitive Flexibility in Aged ApoE4-KI Mice

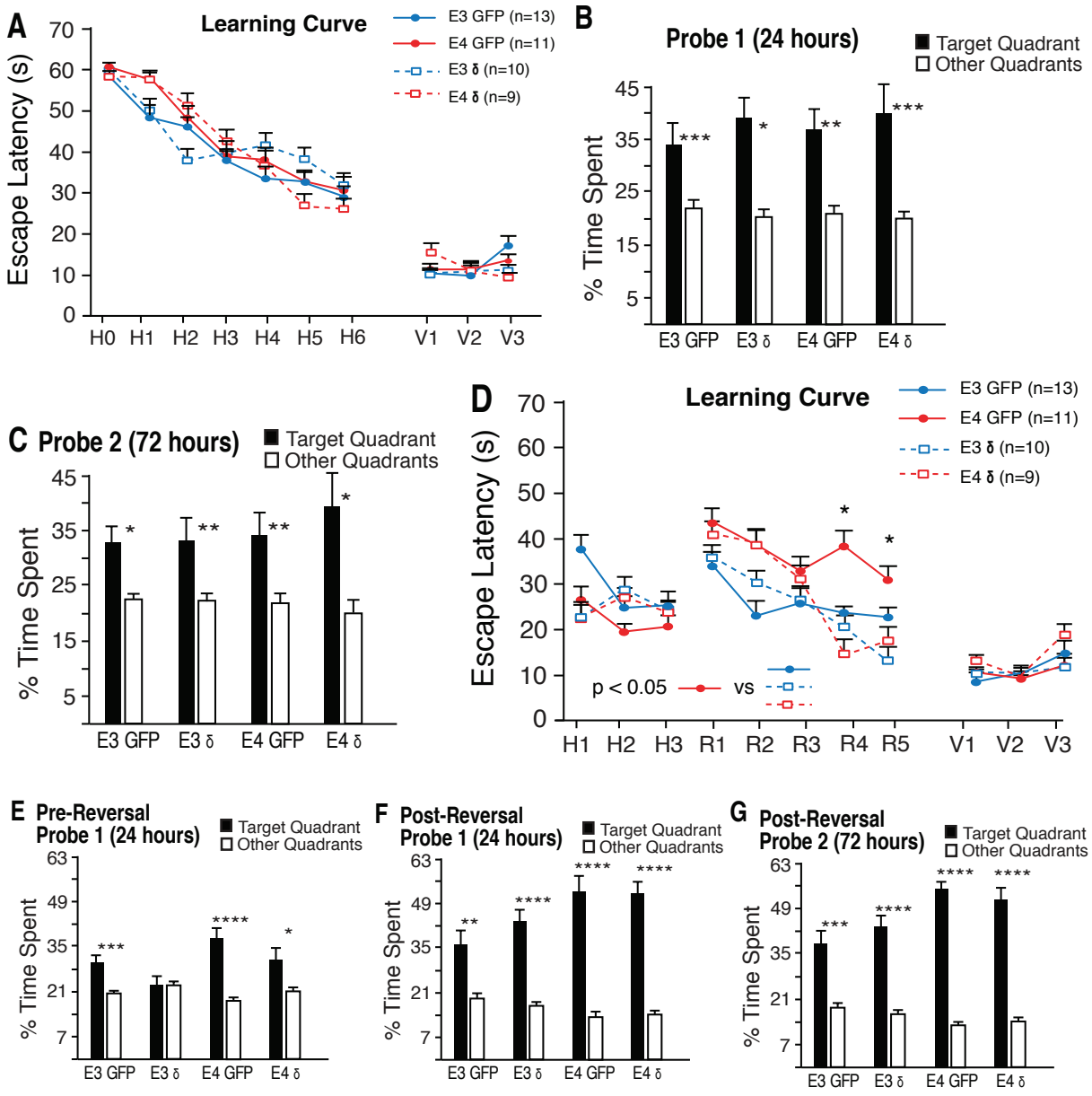

(A) Morris Water Maze results from 17 MO apoE3- and apoE4-KI mice overexpressing GFP or GFP + δ. There was no difference in learning by genotype or overexpression. Points represent averages of daily trials. H, hidden platform day (two trials/session, two sessions/day); H0, first trial on HD1; V, visible platform day (three trials / session, one session). Y axis indicates time to reach the target platform. **(B, C)** All groups showed significant preference for the target quadrant at 24 and 72 hours after final day of training. **(D)** Reversal Morris Water Maze results from cohort used in (A), 6 weeks following the first Morris Water Maze. Mice were trained to find the hidden platform in the original location for three days (H1-3), then platform was moved

to the opposing quadrant and mice were re-trained to find the new platform location for 5 reversal days (R1-5); V, visible platform day (three trials / session, one session). Y axis indicates time to reach the target platform. **(E)** On initial probe performed between H1 and R1, all groups significantly preferred the target quadrant, except E3 overexpressing δ. **(F, G)** In final probes performed after R5, all groups significantly preferred the target quadrant.

Figure 12. Hippocampal Overexpression of $GABA_AR$ Subunit δ Rescues Somatostatin+ Interneuron Numbers in Aged ApoE4-KI Mice

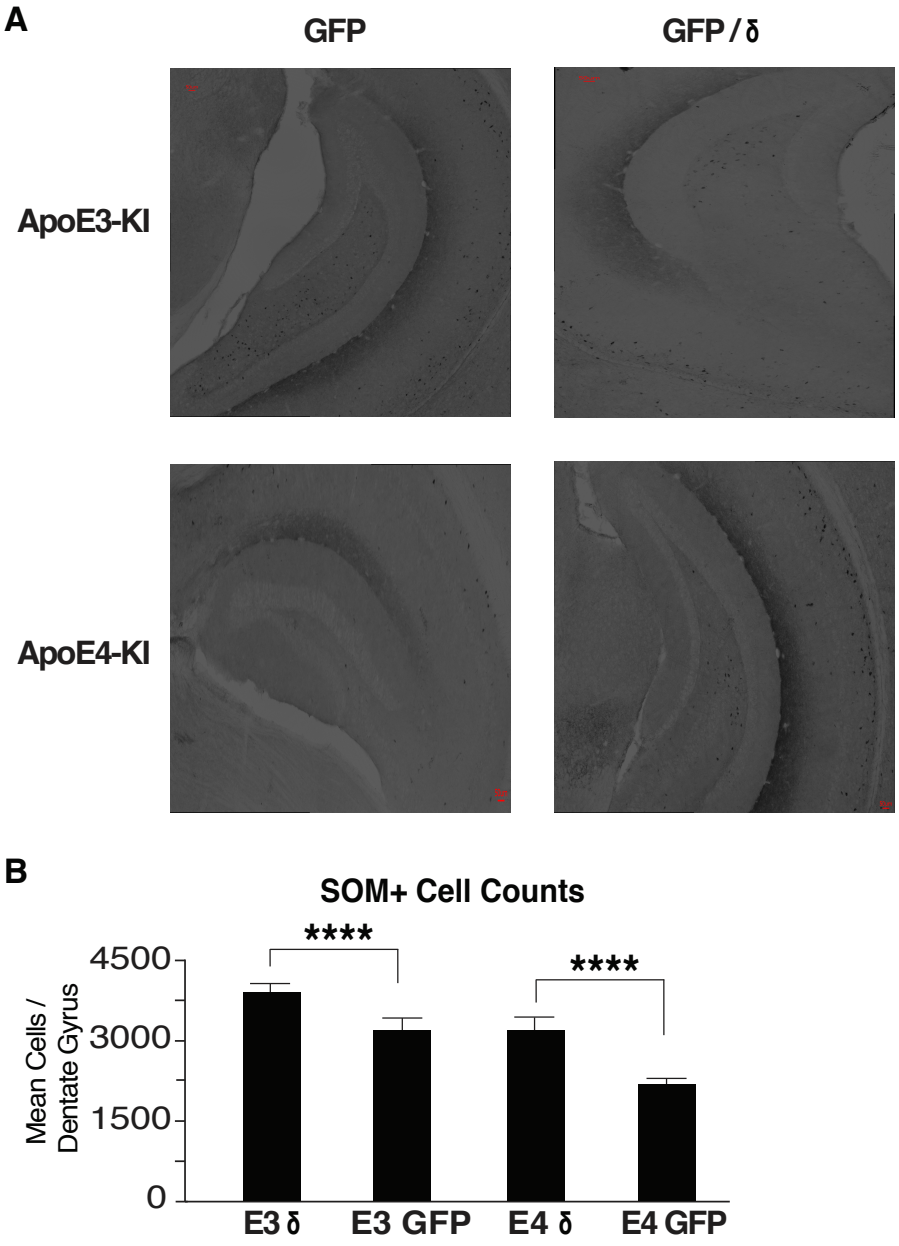

20 MO mice overexpressing either GFP or GFP + δ for 4 months were assessed with floating-section immunohistochemistry. **(A)** Representative images from apoE3- and apoE4-KI overexpressing GFP or GFP + δ, stained for somatostatin (SOM). Every 10th section was saved from the hippocampus, stained, and visible somatostatin-positive (SOM+) interneurons were counted. Total SOM+ count was extrapolated for the hippocampus by multiplying by 10. **(B)**

Quantification of images as in (A). Control apoE4-KI mice had a deficit in SOM+ interneurons relative to apoE3-KI mice, and δ overexpression increased SOM+ counts in both groups.

CHAPTER 5

Discussion and Conclusions

Imbalance between excitation and inhibition in the hippocampus is a feature of AD patients and animal models (Verret et al., 2012; Huang and Mucke 2012). Previous results from our lab have shown that aged female apoE4-KI mice selectively lose GABAergic interneurons in the dentate gyrus (Leung et al., 2012; Andrews-Zwilling et al., 2010), that the extent of this loss correlates with learning and memory deficits (Andrews-Zwilling et al., 2010), and that repopulating dentate gyrus interneurons rescues these deficits (Tong et al., 2014). In this study, we explore two targets that are predicted to increase inhibitory transmission on the *postsynaptic* side (i.e., on primarily excitatory cells that receive inhibitory input) and explore whether manipulating these targets can restore learning and memory. Since we perform these studies in the apoE4-KI model in the context of profound inhibitory interneuron losses, we are essentially asking whether postsynaptic inhibitory increases can compensate for reduced presynaptic inhibitory input.

Increased NKCC1:KCC2 Expression Is a Novel Age- and ApoE4-Related Phenotype

NKCC1 and KCC2 are proteins that import and export chloride anions from neurons (and other cell types, in the case of NKCC1), respectively (Blaesse et al., 2009). Their relative levels of expression and activity contribute to E_{Cl} (Blaesse et al., 2009), which determines E_{GABA}; greater KCC2 (NKCC1) expression leads to more hyperpolarized (depolarized) neuronal response to GABA (Ye et al., 2012). Alterations in the expression levels of these proteins has previously been

associated with temporal epilepsy (Brandt et al., 2010; Palma et al., 2006), among other diseases.

In this study, we provide the first evidence (to our knowledge) of an age-dependent increase in NKCC1 expression, and NKCC1:KCC2 ratio, in the apoE4-KI mouse model. This increase does not appear to be related to the developmental switch from NKCC1 to KCC2 expression, as it is not observed at 2 or 10 months, but is observed by 18 months. ApoE4-KI mice have significant interneuron losses, behavioral deficits, and altered hippocampus-dependent neuronal oscillations (Gillespie, et al. 2016) by 16 months old, raising the possibility that this aberrant expression of NKCC1 is related to these other deficits. The mechanism for the NKCC1 increase remains unknown; it is possible that inhibitory dysfunction itself contributes to CCC expression changes, as appears to be the case in status epilepticus (Pathak et al., 2007), or that some other pathogenic event initiates the increase in NKCC1 levels.

Chronic Bumetanide Treatment Rescues Learning and Memory in Aged ApoE4-KI Mice

Bumetanide is a diuretic drug that selectively inhibits NKCC1 (Hassanejad et al., 2004). Due to the observed increase in NKCC1 in our model, as well as work from other groups demonstrating behavioral rescue from bumetanide in the context of elevated NKCC1 (Deidda et al., 2015), we evaluated bumetanide as a potential therapy for cognitive and behavioral deficits in apoE4-KI mice.

Mice were treated systemically with a low dose of bumetanide (0.2 mg/kg) that had previously been established as effective in other models (Deidda et al., 2015) to have apparent effects within the hippocampus (Sivakumaran and Maguire, 2015). Using two separate cohorts

of aged apoE4-KI mice, we demonstrate that bumetanide treatment normalizes memory in 17 MO mice and learning in 24 MO mice in the Morris Water Maze task. Bumetanide treatment did not affect behavior in the Open Field and Elevated Plus maze tasks, indicating that its cognitive effects are specific to learning and memory. We did not observe any effects in apoE3-KI mice, which is common for treatments that provide behavioral rescue in the apoE4-KI model (see Tong et al., 2014, e.g.). The lack of effect in apoE3-KI mice suggests that bumetanide is not pro-cognitive in general, but acts in a specific disease context – perhaps the context of elevated NKCC1 expression also observed in this study.

$GABA_AR$ Subunit δ Overexpression Improves Cognitive Flexibility, Normalizes Anxiety, and Improves Motor Endurance in Aged ApoE4-KI Mice

δ is one of 19 known subunits that can assemble into the heteropentameric $GABA_ARs$ that mediate the majority of inhibitory transmission in the brain (Whiting, 2003). δ-containing receptors are found largely at extrasynaptic sites and mediate tonic, rather than phasic, inhibition; in the hippocampus, the majority of tonic inhibition is mediated via δ-containing receptors (Chandra et al., 2006; Glykys J et al., 2008; Herd MB et al., 2008). Since tonic inhibition has circuit-stabilizing effects (Walker and Kullman, 2012), we predicted that increasing δ expression might ameliorate inhibitory deficits in apoE4-KI mice, and therefore rescue behavioral deficits.

We used a lentivirus to deliver δ and GFP to dentate gyrus neurons in aged apoE3- and apoE4-KI mice (and GFP only, for control) and used a battery of behavioral tests to determine the consequences. Reversal Morris Water Maze showed that δ overexpression significantly

improved cognitive flexibility in apoE4-KI mice, with no additional effects in apoE3-KI mice. δ overexpression also normalized anxiety-related behavior in apoE4-KI mice to apoE3-like levels. Strikingly (and unexpectedly), δ overexpression also improved performance within the apoE4-KI group in the Rotarod task, a test of motor endurance.

$GABA_AR$ Subunit δ Overexpression Rescues Somatostatin-Positive Interneuron Deficit in Aged ApoE4-KI Mice

ApoE4-KI mice show profound age-dependent inhibitory interneuron losses in the dentate gyrus; there is also a trending decrease in apoE3-KI mice, but the extent is smaller and interneuron numbers do not correlate with learning in this group (Leung et al., 2012). Within the interneuron population, somatostatin-positive cells are selectively lost (Andrews-Zwilling et al., 2010). In this study, δ overexpression increased somatostatin-positive interneurons in the dentate gyrus of both apoE3- and apoE4-KI mice. This observation provides a possible mechanism for the behavioral rescue; however, the relationship between δ, tonic inhibition, and somatostatin interneuron numbers remains a subject for future studies.

Clinical Implications

This set of studies provides a proof-of-concept that postsynaptic inhibitory transmission is an effective drug target in apoE4-related AD, even in the context of profound inhibitory interneuron losses. In the case of δ subunit overexpression, we argue that changes to inhibitory transmission may actually offset these losses. Bumetanide is currently moving into the clinic for several neurological diseases, and we advocate that further preclinical studies be performed for

bumetanide in the context of AD, with the ultimate goal of assessing bumetanide as a treatment for apoE4-related AD. This work also supports δ as a candidate drug target in AD.

CHAPTER 6

Future Directions

As there are currently no effective disease-modifying therapeutics for AD, there is an urgent need to translate promising candidates to the clinic (Huang & Mucke, 2012). This study demonstrates that bumetanide is effective for reducing the cognitive symptoms of AD in apoE4-related AD. Since bumetanide is an FDA-approved treatment in the United States, that has allowed rapid translation from animal studies to case reports and small clinical trials in humans (e.g. for autism: Hadjikhani et al., 2015). Before translation is attempted, however, more work is needed to understand whether bumetanide rescues cognition in AD in general, or whether it specifically acts in the apoE4 context. Studies using other major models of AD, incorporating pathogenic expression of Aβ and tau, should address this.

In addition, the mechanism by which bumetanide acts in AD is poorly understood. This work has suggested that changes in CCC protein expression may be involved, but the full picture is likely to involve gene expression and functional changes as well. Gene expression changes could be explored in animal models or primary neurons. Our group is currently performing RNA sequencing on dissociated hippocampal cells from aged apoE3- and apoE4-KI mice treated with bumetanide by i.p., as well as on human neurons derived from stem cells expressing ApoE4. These studies should answer whether bumetanide normalizes the gene expression signature of ApoE4-related AD. Additional studies, such as perforated-patch *in vitro* physiology and cortical EEG, should explore the functional effects of bumetanide administration on apoE4-KI mice.

The relationship between the observed increase in NKCC1 expression in apoE4-KI mice and the other phenotypes observed at old age in this model – including learning and memory

deficits, altered hippocampal-dependent neuronal oscillations, and interneuron losses – remains unknown. The Dlx/E4-fKI model appears to be negative for all of these phenotypes, additionally suggesting a relationship between them, but leaving the causality unknown. Future studies should seek to untangle the causal relationships between these observed phenotypes. One simple means for addressing this would be to fill in the time points between 10 and 18 months and assessing NKCC1 expression at these times. The failure of pentobarbital treatment to lower NKCC1 expression suggests that NKCC1 protein levels do not immediately respond to changes in neuronal inhibition, but this is not conclusive as the time scale (2 weeks) was relatively short; it would be illuminating to examine NKCC1 levels in apoE4-KI mice that were treated prophylactically with pentobarbital, or that had their interneuron population replaced via transplantation. It is also unknown whether bumetanide could be used prophylactically, before interneuron losses and behavioral deficits emerge, or whether it is only effective in the context of disease.

Bumetanide is a promising treatment for many neurological diseases and has acute and disease-modifying effects in TLE even at low doses (Brandt et al., 2010). However, it has a short half-life and is poorly bioavailable (Lee et al., 1994). There is also evidence that its main side effect, diuresis, is more pronounced in humans than rodents (Romanova et al., 1985), so it is possible that animal studies underestimate its adverse effects. Therefore, it would be desirable to engineer a form of bumetanide that is optimized for delivery to the brain. Work is currently underway to develop new “prodrugs” of bumetanide that will better penetrate the blood-brain barrier (Töllner et al., 2015). As bumetanide continues to advance in clinical trials for various neurological diseases, these newer NKCC1 inhibitors should be considered in parallel for their

potentially enhanced efficacy and reduced side effects. However, bumetanide is approved for human use by the FDA, so these newer compounds may present regulatory challenges.

$GABA_AR$ subunit δ also appears to be a promising drug target for apoE4-related AD with both cognitive and potentially neuroprotective effects. More work is required to understand the mechanism by which δ exerts these beneficial effects. Since δ itself contributes to tonic inhibition, slice physiology experiments are currently underway in apoE4-KI mice to explore whether apoE4 causes a deficit in tonic inhibition, and whether overexpression of δ enhances tonic inhibition in these animals. *In vivo* electrophysiology should also be pursued to understand whether δ impacts the known oscillatory deficits in the apoE4-KI model (Gillespie et al., 2016), as local changes to tonic inhibition may have a circuit-stabilizing effect. In addition to advancing understanding of AD, this work would contribute to the theoretical understanding of memory encoding in the hippocampus, and the critical role of neuronal inhibition in hippocampal function.

There are several compounds that act on $GABA_AR$ subunit δ. The most widely-studied is known as Gaboxadol or 4,5,6,7-tetrahydroisoxazolo(5,4-c)pyridin-3-ol (THIP). While it is widely noted that THIP has greater agonist effects at δ-containing receptors than γ_2-containing receptors (Meera et al., 2011), THIP is actually anti-selective for the γ_2 subunit (Shu et al., 2002) (which does not form receptors with δ *in vivo*), not truly δ-selective. THIP was evaluated as an early AD therapy, but was abandoned due to low efficacy in initial clinical studies (Mohr et al., 1986); it has more recently been pursued as a treatment for insomnia due to its hypnotic "side effect" (Krogsgaard-Larsen et al., 2004). Its sedative effect likely indicates an off-target effect outside the hippocampus. Therefore, it would be desirable to develop a truly selective δ-acting

compound. One such compound, DS2, has recently been identified as a *bona fide* δ potentiator (Wafford et al., 2009). DS2 is also partially selective for the α subunit, with even greater activity at the $\alpha_4\beta\delta$ receptor found in the dentate gyrus than other δ-containing receptors (Lee et al., 2016), and enhances tonic inhibition in dentate gyrus granule cells (Carver & Reddy, 2016). DS2 may therefore hold promise as a treatment for ApoE4-related AD.

Finally, we predicted that the two therapies explored in this paper – bumetanide and δ – act via modulating postsynaptic inhibition. While a reasonable prediction, further studies are needed to confirm that this is the case. Bumetanide is well-established to hyperpolarize E_{Cl} in neurons, but this has not been conclusively shown in the apoE4-KI model. Since apoE4-KI deficits appear with age, the effect of bumetanide on E_{Cl} would also need to be performed on aged mice, which is a significant technical challenge for *in vitro* electrophysiology – though not an insurmountable one. In the case of δ, we are currently working to confirm that δ overexpression increases tonic inhibition in dentate gyrus granule cells using patch clamp electrophysiology.

REFERENCES

Andrews-Zwilling, Y., Bien-Ly, N., Xu, Q., Li, G., Bernardo, A., Yoon, S. Y., ... & Huang, Y. (2010). Apolipoprotein E4 causes age-and Tau-dependent impairment of GABAergic interneurons, leading to learning and memory deficits in mice. Journal of Neuroscience, 30(41), 13707-13717.

Andrews-Zwilling, Y., Gillespie, A. K., Kravitz, A. V., Nelson, A. B., Devidze, N., Lo, I., ... & Potter, G. B. (2012). Hilar GABAergic interneuron activity controls spatial learning and memory retrieval. PloS one, 7(7), e40555.

Aronica, E., Boer, K., Redeker, S., Spliet, W. G. M., Van Rijen, P. C., Troost, D., & Gorter, J. A. (2007). Differential expression patterns of chloride transporters, Na+-K+-2Cl−-cotransporter and K+-Cl−-cotransporter, in epilepsy-associated malformations of cortical development. Neuroscience, 145(1), 185-196.

Bakker, A., Krauss, G. L., Albert, M. S., Speck, C. L., Jones, L. R., Stark, C. E., ... & Gallagher, M. (2012). Reduction of hippocampal hyperactivity improves cognition in amnestic mild cognitive impairment. Neuron, 74(3), 467-474.

Ball, M. J., Hachinski, V., Fox, A., Kirshen, A. J., Fisman, M., Blume, W., ... & Merskey, H. (1985). A new definition of Alzheimer's disease: a hippocampal dementia. The Lancet, 325(8419), 14-16.

Barnes, D. E., & Yaffe, K. (2011). The projected effect of risk factor reduction on Alzheimer's disease prevalence. The Lancet Neurology, 10(9), 819-828.

Beck, J., Lenart, B., Kintner, D. B., & Sun, D. (2003). Na-K-Cl cotransporter contributes to glutamate-mediated excitotoxicity. Journal of Neuroscience, 23(12), 5061-5068.

Belelli, D., & Lambert, J. J. (2005). Neurosteroids: endogenous regulators of the GABAA receptor. Nature Reviews Neuroscience, 6(7), 565-575.

Ben-Ari, Y. (2015). Is birth a critical period in the pathogenesis of autism spectrum disorders?. Nature Reviews Neuroscience, 16(8), 498-505.

Ben-Ari, Y., Damier, P., & Lemonnier, E. (2016). Failure of the Nemo Trial: Bumetanide Is a Promising Agent to Treat Many Brain Disorders but Not Newborn Seizures. Frontiers in cellular neuroscience, 10.

Berchtold, N. C., Coleman, P. D., Cribbs, D. H., Rogers, J., Gillen, D. L., & Cotman, C. W. (2013). Synaptic genes are extensively downregulated across multiple brain regions in normal human aging and Alzheimer's disease. Neurobiology of aging, 34(6), 1653-1661.

Berron, D., Schütze, H., Maass, A., Cardenas-Blanco, A., Kuijf, H. J., Kumaran, D., & Düzel, E. (2016). Strong evidence for pattern separation in human dentate gyrus. Journal of Neuroscience, 36(29), 7569-7579.

Bertram, L., Lill, C. M., & Tanzi, R. E. (2010). The genetics of Alzheimer disease: back to the future. Neuron, 68(2), 270-281.

Bien-Ly, N., Gillespie, A. K., Walker, D., Yoon, S. Y., & Huang, Y. (2012). Reducing human apolipoprotein E levels attenuates age-dependent Aβ accumulation in mutant human amyloid precursor protein transgenic mice. Journal of Neuroscience, 32(14), 4803-4811.

Blaesse, P., Airaksinen, M. S., Rivera, C., & Kaila, K. (2009). Cation-chloride cotransporters and neuronal function. Neuron, 61(6), 820-838.

Blennow, K., de Leon, M. J., Zetterberg, H. (2006). Alzheimer's Disease. The Lancet, 368(9533), 387-403.

Bloom, G. S. (2014). Amyloid-β and tau: the trigger and bullet in Alzheimer disease pathogenesis. JAMA neurology, 71(4), 505-508.

Bookheimer, S. Y., Strojwas, M. H., Cohen, M. S., Saunders, A. M., Pericak-Vance, M. A., Mazziotta, J. C., & Small, G. W. (2000). Patterns of brain activation in people at risk for Alzheimer's disease. New England journal of medicine, 343(7), 450-456.

Bourke, E., Asbury, M. J. A., O'Sullivan, S., & Gatenby, P. B. B. (1973). The sites of action of bumetanide in man. European journal of pharmacology, 23(3), 283-289.

Bradshaw, J., Saling, M., Hopwood, M., Anderson, V., & Brodtmann, A. (2004). Fluctuating cognition in dementia with Lewy bodies and Alzheimer's disease is qualitatively distinct. Journal of Neurology, Neurosurgery & Psychiatry, 75(3), 382-387.

Brandt, C., Nozadze, M., Heuchert, N., Rattka, M., & Löscher, W. (2010). Disease-modifying effects of phenobarbital and the NKCC1 inhibitor bumetanide in the pilocarpine model of temporal lobe epilepsy. Journal of Neuroscience, 30(25), 8602-8612.

Brater, D. C., Day, B., Burdette, A., & Anderson, S. (1984). Bumetanide and furosemide in heart failure. Kidney international, 26(2), 183-189.

Brecht, W. J., Harris, F. M., Chang, S., Tesseur, I., Yu, G. Q., Xu, Q., ... & Mahley, R. W. (2004). Neuron-specific apolipoprotein e4 proteolysis is associated with increased tau phosphorylation in brains of transgenic mice. Journal of Neuroscience, 24(10), 2527-2534.

Carver, C. M., & Reddy, D. S. (2016). Neurosteroid Structure-Activity Relationships for Functional Activation of Extrasynaptic δGABAA Receptors. Journal of Pharmacology and Experimental Therapeutics, 357(1), 188-204.

Celone, K. A., Calhoun, V. D., Dickerson, B. C., Atri, A., Chua, E. F., Miller, S. L., ... & Albert, M. S. (2006). Alterations in memory networks in mild cognitive impairment and Alzheimer's disease: an independent component analysis. Journal of Neuroscience, 26(40), 10222-10231.

Chandra, D., Jia, F., Liang, J., Peng, Z., Suryanarayanan, A., Werner, D. F., ... & Homanics, G. E. (2006). GABAA receptor α4 subunits mediate extrasynaptic inhibition in thalamus and dentate gyrus and the action of gaboxadol. Proceedings of the National Academy of Sciences, 103(41), 15230-15235.

Chang, S., ran Ma, T., Miranda, R. D., Balestra, M. E., Mahley, R. W., & Huang, Y. (2005). Lipid- and receptor-binding regions of apolipoprotein E4 fragments act in concert to cause mitochondrial dysfunction and neurotoxicity. Proceedings of the National Academy of Sciences of the United States of America, 102(51), 18694-18699.

Cherubini, E., Griguoli, M., Safiulina, V., & Lagostena, L. (2011). The depolarizing action of GABA controls early network activity in the developing hippocampus. Molecular neurobiology, 43(2), 97-106.

Cleary, R. T., Sun, H., Huynh, T., Manning, S. M., Li, Y., Rotenberg, A., ... & Berry, G. (2013). Bumetanide enhances phenobarbital efficacy in a rat model of hypoxic neonatal seizures. PLoS One, 8(3), e57148.

Coppedè, F., & Migliore, L. (2009). DNA damage and repair in Alzheimer's disease. Current Alzheimer Research, 6(1), 36-47.

Costes, S. V., Daelemans, D., Cho, E. H., Dobbin, Z., Pavlakis, G., & Lockett, S. (2004). Automatic and quantitative measurement of protein-protein colocalization in live cells. Biophysical journal, 86(6), 3993-4003.

Damier, P., Hammond, C., & Ben-Ari, Y. (2016). Bumetanide to treat parkinson disease: a report of 4 cases. Clinical neuropharmacology, 39(1), 57-59.

Das, U., Scott, D. A., Ganguly, A., Koo, E. H., Tang, Y., & Roy, S. (2013). Activity-induced convergence of APP and BACE-1 in acidic microdomains via an endocytosis-dependent pathway. Neuron, 79(3), 447-460.

de Gage, S. B., Bégaud, B., Bazin, F., Verdoux, H., Dartigues, J. F., Pérès, K., ... & Pariente, A. (2012). Benzodiazepine use and risk of dementia: prospective population based study. BMJ, 345, e6231.

Dehorter, N., Lozovaya, N., Mdzomba, B. J., Michel, F. J., Lopez, C., Tsintsadze, V., ... & Hammond, C. (2012). Subthalamic lesion or levodopa treatment rescues giant GABAergic currents of PINK1-deficient striatum. Journal of Neuroscience, 32(50), 18047-18053.

Deidda, G., Parrini, M., Naskar, S., Bozarth, I. F., Contestabile, A., & Cancedda, L. (2015). Reversing excitatory GABAAR signaling restores synaptic plasticity and memory in a mouse model of Down syndrome. Nature medicine, 21(4), 318-326.

Dickerson, B. C., & Sperling, R. A. (2008). Functional abnormalities of the medial temporal lobe memory system in mild cognitive impairment and Alzheimer's disease: insights from functional MRI studies. Neuropsychologia, 46(6), 1624-1635.

Dzhala, V. I., Brumback, A. C., & Staley, K. J. (2008). Bumetanide enhances phenobarbital efficacy in a neonatal seizure model. Annals of neurology, 63(2), 222-235.

Dzhala, V. I., Talos, D. M., Sdrulla, D. A., Brumback, A. C., Mathews, G. C., Benke, T. A., ... & Staley, K. J. (2005). NKCC1 transporter facilitates seizures in the developing brain. Nature medicine, 11(11), 1205-1213.

Farrant, M., & Nusser, Z. (2005). Variations on an inhibitory theme: phasic and tonic activation of GABAA receptors. Nature Reviews Neuroscience, 6(3), 215-229.

Farrer, L. A., Cupples, L. A., Haines, J. L., Hyman, B., Kukull, W. A., Mayeux, R., ... & Van Duijn, C. M. (1997). Effects of age, sex, and ethnicity on the association between apolipoprotein E genotype and Alzheimer disease: a meta-analysis. Jama, 278(16), 1349-1356.

Feng, H. J., Bianchi, M. T., & Macdonald, R. L. (2004). Pentobarbital differentially modulates α1β3δ and α1β3γ2L GABAA receptor currents. Molecular pharmacology, 66(4), 988-1003.

Flagella, M., Clarke, L. L., Miller, M. L., Erway, L. C., Giannella, R. A., Andringa, A., ... & Lorenz, J. N. (1999). Mice lacking the basolateral Na-K-2Cl cotransporter have impaired epithelial chloride secretion and are profoundly deaf. Journal of Biological Chemistry, 274(38), 26946-26955.

Flamenbaum, W., & Friedman, R. (1982). Pharmacology, therapeutic efficacy, and adverse effects of bumetanide, a new “loop” diuretic. Pharmacotherapy: The Journal of Human Pharmacology and Drug Therapy, 2(4), 213-222.

Frederikse, P. H., & Kasinathan, C. (2015). KCC2 expression supersedes NKCC1 in mature fiber cells in mouse and rabbit lenses. Molecular vision, 21, 1142.

Ganguly, K., Schinder, A. F., Wong, S. T., & Poo, M. M. (2001). GABA itself promotes the developmental switch of neuronal GABAergic responses from excitation to inhibition. Cell, 105(4), 521-532.

Gao, R., & Penzes, P. (2015). Common mechanisms of excitatory and inhibitory imbalance in schizophrenia and autism spectrum disorders. Current molecular medicine, 15(2), 146-167.

Genin, E., Hannequin, D., Wallon, D., Sleegers, K., Hiltunen, M., Combarros, O., ... & Pasquier, F. (2011). APOE and Alzheimer disease: a major gene with semi-dominant inheritance. Molecular psychiatry, 16(9), 903-907.

Giannakopoulos, P., Herrmann, F. R., Bussiere, T., Bouras, C., Kövari, E., Perl, D. P., ... & Hof, P. R. (2003). Tangle and neuron numbers, but not amyloid load, predict cognitive status in Alzheimer's disease. Neurology, 60(9), 1495-1500.

Gilbert, P. E., Kesner, R. P., & Lee, I. (2001). Dissociating hippocampal subregions: A double dissociation between dentate gyrus and CA1. Hippocampus, 11(6), 626-636.

Gillespie, A. K., Jones, E. A., Lin, Y. H., Karlsson, M. P., Kay, K., Yoon, S. Y., ... & Huang, Y. (2016). Apolipoprotein E4 causes age-dependent disruption of slow gamma oscillations during hippocampal sharp-wave ripples. Neuron, 90(4), 740-751.

Glykys, J., Mann, E. O., & Mody, I. (2008). Which GABAA receptor subunits are necessary for tonic inhibition in the hippocampus?. Journal of Neuroscience, 28(6), 1421-1426.

Golde, T. E., Schneider, L. S., & Koo, E. H. (2011). Anti-aβ therapeutics in Alzheimer's disease: the need for a paradigm shift. Neuron, 69(2), 203-213.

Gómez-Isla, T., Price, J. L., McKeel Jr, D. W., Morris, J. C., Growdon, J. H., & Hyman, B. T. (1996). Profound loss of layer II entorhinal cortex neurons occurs in very mild Alzheimer's disease. Journal of Neuroscience, 16(14), 4491-4500.

Gould, T. D., Dao, D. T., & Kovacsics, C. E. (2009). The open field test. Mood and anxiety related phenotypes in mice: Characterization using behavioral tests, 1-20.

Greicius, M. D., Srivastava, G., Reiss, A. L., & Menon, V. (2004). Default-mode network activity distinguishes Alzheimer's disease from healthy aging: evidence from functional MRI. Proceedings of the National Academy of Sciences of the United States of America, 101(13), 4637-4642.

Haas, M. A. R. K., & McMANUS, T. J. (1983). Bumetanide inhibits (Na+ K+ 2Cl) co-transport at a chloride site. American Journal of Physiology-Cell Physiology, 245(3), C235-C240.

Haass, C., Schlossmacher, M. G., Hung, A. Y., Vigo-Pelfrey, C., Mellon, A., Ostaszewski, B. L., ... & Teplow, D. B. (1992). Amyloid beta-peptide is produced by cultured cells during normal metabolism. Nature, 359(6393), 322.

Hadjikhani, N., Zürcher, N. R., Rogier, O., Ruest, T., Hippolyte, L., Ben-Ari, Y., & Lemonnier, E. (2015). Improving emotional face perception in autism with diuretic bumetanide: a proof-of-concept behavioral and functional brain imaging pilot study. Autism, 19(2), 149-157.

Hamanaka, H., Katoh-Fukui, Y., Suzuki, K., Kobayashi, M., Suzuki, R., Motegi, Y., ... & Yokoyama, M. (2000). Altered cholesterol metabolism in human apolipoprotein E4 knock-in mice. Human molecular genetics, 9(3), 353-361.

Hardy, J., & Selkoe, D. J. (2002). The amyloid hypothesis of Alzheimer's disease: progress and problems on the road to therapeutics. science, 297(5580), 353-356.

Hasannejad, H., Takeda, M., Taki, K., Shin, H. J., Babu, E., Jutabha, P., ... & Enomoto, A. (2004). Interactions of human organic anion transporters with diuretics. Journal of Pharmacology and Experimental Therapeutics, 308(3), 1021-1029.

He, Q., Nomura, T., Xu, J., & Contractor, A. (2014). The developmental switch in GABA polarity is delayed in fragile X mice. Journal of Neuroscience, 34(2), 446-450.

Hekmat-Scafe, D. S., Lundy, M. Y., Ranga, R., & Tanouye, M. A. (2006). Mutations in the K+/Cl− cotransporter gene kazachoc (kcc) increase seizure susceptibility in Drosophila. Journal of Neuroscience, 26(35), 8943-8954.

Herd, M. B., Haythornthwaite, A. R., Rosahl, T. W., Wafford, K. A., Homanics, G. E., Lambert, J. J., & Belelli, D. (2008). The expression of GABAAβ subunit isoforms in synaptic and extrasynaptic receptor populations of mouse dentate gyrus granule cells. The Journal of physiology, 586(4), 989-1004.

Holtzman, D. M., Pitas, R. E., Kilbridge, J., Nathan, B., Mahley, R. W., Bu, G., & Schwartz, A. L. (1995). Low density lipoprotein receptor-related protein mediates apolipoprotein E-dependent neurite outgrowth in a central nervous system-derived neuronal cell line. Proceedings of the National Academy of Sciences, 92(21), 9480-9484.

Huang, Y. (2006). Molecular and cellular mechanisms of apolipoprotein E4 neurotoxicity and potential therapeutic strategies. Current opinion in drug discovery & development, 9(5), 627-641.

Huang, Y., & Mucke, L. (2012). Alzheimer mechanisms and therapeutic strategies. Cell, 148(6), 1204-1222.

Hyde, T. M., Lipska, B. K., Ali, T., Mathew, S. V., Law, A. J., Metitiri, O. E., ... & Bigelow, L. B. (2011). Expression of GABA signaling molecules KCC2, NKCC1, and GAD1 in cortical development and schizophrenia. Journal of Neuroscience, 31(30), 11088-11095.

Hynd, M. R., Scott, H. L., & Dodd, P. R. (2004). Glutamate-mediated excitotoxicity and neurodegeneration in Alzheimer's disease. Neurochemistry international, 45(5), 583-595.

Imai, M. (1977). Effect of bumetanide and furosemide on the thick ascending limb of Henle's loop of rabbits and rats perfused in vitro. European journal of pharmacology, 41(4), 409-416.

Jedlicka, P., Owen, M., Vnencak, M., Tschäpe, J. A., Hick, M., Müller, U. C., & Deller, T. (2012). Functional consequences of the lack of amyloid precursor protein in the mouse dentate gyrus in vivo. Experimental brain research, 217(3-4), 441-447.

Jensen, M. L., Wafford, K. A., Brown, A. R., Belelli, D., Lambert, J. J., & Mirza, N. R. (2013). A study of subunit selectivity, mechanism and site of action of the delta selective compound 2 (DS2) at human recombinant and rodent native GABAA receptors. British journal of pharmacology, 168(5), 1118-1132.

Jimenez-Jimenez, F. J., Molina, J. A., Gomez, P., Vargas, C., De Bustos, F., Benito-Leon, J., ... & Arenas, J. (1998). Neurotransmitter amino acids in cerebrospinal fluid of patients with Alzheimer's disease. Journal of neural transmission, 105(2), 269-277.

Jones, B. J., & Roberts, D. J. (1968). The quantitative measurement of motor inco-ordination in naive mice using an accelerating rotarod. Journal of Pharmacy and Pharmacology, 20(4), 302-304.

Kahle, K. T., Staley, K. J., Nahed, B. V., Gamba, G., Hebert, S. C., Lifton, R. P., & Mount, D. B. (2008). Roles of the cation–chloride cotransporters in neurological disease. Nature Clinical Practice Neurology, 4(9), 490-503.

Kaila, K., Price, T. J., Payne, J. A., Puskarjov, M., & Voipio, J. (2014). Cation-chloride cotransporters in neuronal development, plasticity and disease. Nature Reviews Neuroscience, 15(10), 637-654.

Kim, J., Basak, J. M., & Holtzman, D. M. (2009). The role of apolipoprotein E in Alzheimer's disease. Neuron, 63(3), 287-303.

Korpi, E. R., Gründer, G., & Lüddens, H. (2002). Drug interactions at GABA A receptors. Progress in neurobiology, 67(2), 113-159.

Krogsgaard-Larsen, P., Frølund, B., Liljefors, T., & Ebert, B. (2004). GABA A agonists and partial agonists: THIP (Gaboxadol) as a non-opioid analgesic and a novel type of hypnotic. Biochemical pharmacology, 68(8), 1573-1580.

Krstic, D., & Knuesel, I. (2013). The airbag problem–a potential culprit for bench-to-bedside translational efforts: relevance for Alzheimer's disease. Acta neuropathologica communications, 1(1), 62.

Kunz, L., Schröder, T. N., Lee, H., Montag, C., Lachmann, B., Sariyska, R., ... & Fell, J. (2015). Reduced grid-cell–like representations in adults at genetic risk for Alzheimer's disease. Science, 350(6259), 430-433.

Larner, A. J. (2010). Epileptic seizures in AD patients. Neuromolecular medicine, 12(1), 71-77.

Lee, H. J., Absalom, N. L., Hanrahan, J. R., van Nieuwenhuijzen, P., Ahring, P. K., & Chebib, M. (2016). A pharmacological characterization of GABA, THIP and DS2 at binary α4β3 and β3δ receptors: GABA activates β3δ receptors via the β3 (+) δ (−) interface. Brain research, 1644, 222-230.

Lee, S. H., Lee, M. G., & Kim, N. D. (1994). Pharmacokinetics and pharmacodynamics of bumetanide after intravenous and oral administration to rats: absorption from various GI segments. Journal of pharmacokinetics and biopharmaceutics, 22(1), 1-17.

Lein, E. S., Hawrylycz, M. J., Ao, N., Ayres, M., Bensinger, A., Bernard, A., ... & Chen, L. (2007). Genome-wide atlas of gene expression in the adult mouse brain. Nature, 445(7124), 168-176.

Lemonnier, É., Degrez, C., Phelep, M., Tyzio, R., Josse, F., Grandgeorge, M., ... & Ben-Ari, Y. (2012). A randomised controlled trial of bumetanide in the treatment of autism in children. Translational psychiatry, 2(12), e202.

Lemonnier, E., Lazartigues, A., & Ben-Ari, Y. (2016). Treating schizophrenia with the diuretic bumetanide: a case report. Clinical neuropharmacology, 39(2), 115-117.

Leung, L., Andrews-Zwilling, Y., Yoon, S. Y., Jain, S., Ring, K., Dai, J., ... & Huang, Y. (2012). Apolipoprotein E4 causes age-and sex-dependent impairments of hilar GABAergic interneurons and learning and memory deficits in mice. PloS one, 7(12), e53569.

Leutgeb, J. K., Leutgeb, S., Moser, M. B., & Moser, E. I. (2007). Pattern separation in the dentate gyrus and CA3 of the hippocampus. science, 315(5814), 961-966.

Lin, M. T., & Beal, M. F. (2006). Mitochondrial dysfunction and oxidative stress in neurodegenerative diseases. Nature, 443(7113), 787-795.

Luscher, B., Fuchs, T., & Kilpatrick, C. L. (2011). GABA A receptor trafficking-mediated plasticity of inhibitory synapses. Neuron, 70(3), 385-409.

Maguire, J., & Mody, I. (2009). Steroid hormone fluctuations and GABA A R plasticity. Psychoneuroendocrinology, 34, S84-S90.

Maguire, J. L., Stell, B. M., Rafizadeh, M., & Mody, I. (2005). Ovarian cycle–linked changes in GABAA receptors mediating tonic inhibition alter seizure susceptibility and anxiety. Nature neuroscience, 8(6), 797-804.

Mahley, R. W. (1988). Apolipoprotein E: cholesterol transport protein with expanding role in cell biology. Science, 240(4852), 622.

Mahley, R. W., Weisgraber, K. H., & Huang, Y. (2006). Apolipoprotein E4: a causative factor and therapeutic target in neuropathology, including Alzheimer's disease. Proceedings of the National Academy of Sciences, 103(15), 5644-5651.

Mangialasche, F., Solomon, A., Winblad, B., Mecocci, P., & Kivipelto, M. (2010). Alzheimer's disease: clinical trials and drug development. The Lancet Neurology, 9(7), 702-716.

Marín, O. (2012). Interneuron dysfunction in psychiatric disorders. Nature Reviews Neuroscience, 13(2), 107-120.

McGahan, M. C., Yorio, T., & Bentley, P. J. (1977). The mode of action of bumetanide: inhibition of chloride transport across the amphibian cornea. Journal of Pharmacology and Experimental Therapeutics, 203(1), 97-102.

Meera, P., Wallner, M., & Otis, T. S. (2011). Molecular basis for the high THIP/gaboxadol sensitivity of extrasynaptic GABAA receptors. Journal of neurophysiology, 106(4), 2057-2064.

Mody, I. (2001). Distinguishing between GABAA receptors responsible for tonic and phasic conductances. Neurochemical research, 26(8), 907-913.

Mohr, E., Bruno, G., Foster, N., Gillespie, M., Cox, C., Hare, T. A., ... & Chase, T. N. (1986). GABA-agonist therapy for Alzheimer's disease. Clinical neuropharmacology, 9(3), 257-263.

Morgan, R. J., Santhakumar, V., & Soltesz, I. (2007). Modeling the dentate gyrus. Progress in brain research, 163, 639-658.

Morris, R. (1984). Developments of a water-maze procedure for studying spatial learning in the rat. Journal of neuroscience methods, 11(1), 47-60.

Mortensen, M., & Smart, T. G. (2006). Extrasynaptic αβ subunit GABAA receptors on rat hippocampal pyramidal neurons. The Journal of physiology, 577(3), 841-856.

Murphy, G. G. (2013). Spatial learning and memory—what's TLE got to do with it? Epilepsy Currents, 13(1), 26-29.

Myers, C. E., & Scharfman, H. E. (2009). A role for hilar cells in pattern separation in the dentate gyrus: a computational approach. Hippocampus, 19(4), 321-337.

Nardou, R., Ben-Ari, Y., & Khalilov, I. (2009). Bumetanide, an NKCC1 antagonist, does not prevent formation of epileptogenic focus but blocks epileptic focus seizures in immature rat hippocampus. Journal of neurophysiology, 101(6), 2878-2888.

Olsen, R. W., Delorey, T. M., Handforth, A., Ferguson, C., Mihalek, R. M., & Homanics, G. E. (1997). Epilepsy In Mice Lacking Gaba-receptor Delta (d) Subunits. Epilepsia, 38, 123.

Ong, W. Y., Tanaka, K., Dawe, G. S., Ittner, L. M., & Farooqui, A. A. (2013). Slow excitotoxicity in Alzheimer's disease. Journal of Alzheimer's Disease, 35(4), 643-668.

Palma, E., Amici, M., Sobrero, F., Spinelli, G., Di Angelantonio, S., Ragozzino, D., ... & Eusebi, F. (2006). Anomalous levels of Cl− transporters in the hippocampal subiculum from temporal lobe epilepsy patients make GABA excitatory. Proceedings of the National Academy of Sciences, 103(22), 8465-8468.

Palop, J. J., & Mucke, L. (2009). Epilepsy and cognitive impairments in Alzheimer disease. Archives of neurology, 66(4), 435-440.

Palop, J. J., & Mucke, L. (2010). Amyloid-[beta]-induced neuronal dysfunction in Alzheimer's disease: from synapses toward neural networks. Nature neuroscience, 13(7), 812-818.

Palop, J. J., Chin, J., & Mucke, L. (2006). A network dysfunction perspective on neurodegenerative diseases. Nature, 443(7113), 768-773.

Palop, J. J., Chin, J., Roberson, E. D., Wang, J., Thwin, M. T., Bien-Ly, N., ... & Finkbeiner, S. (2007). Aberrant excitatory neuronal activity and compensatory remodeling of inhibitory hippocampal circuits in mouse models of Alzheimer's disease. Neuron, 55(5), 697-711.

Pathak, H. R., Weissinger, F., Terunuma, M., Carlson, G. C., Hsu, F. C., Moss, S. J., & Coulter, D. A. (2007). Disrupted dentate granule cell chloride regulation enhances synaptic excitability during development of temporal lobe epilepsy. Journal of Neuroscience, 27(51), 14012-14022.

Payne, J. A., Rivera, C., Voipio, J., & Kaila, K. (2003). Cation–chloride co-transporters in neuronal communication, development and trauma. Trends in neurosciences, 26(4), 199-206.

Pentikainen, P. J., Penttila, A. N. E. R. I., Neuvonen, P. J., & Gothoni, G. (1977). Fate of [14C]-bumetanide in man. British journal of clinical pharmacology, 4(1), 39-44.

Petrini, E. M., Marchionni, I., Zacchi, P., Sieghart, W., & Cherubini, E. (2004). Clustering of extrasynaptic GABAA receptors modulates tonic inhibition in cultured hippocampal neurons. Journal of Biological Chemistry, 279(44), 45833-45843.

Pirker, S., Schwarzer, C., Wieselthaler, A., Sieghart, W., & Sperk, G. (2000). GABA A receptors: immunocytochemical distribution of 13 subunits in the adult rat brain. Neuroscience, 101(4), 815-850.

Potter, G. B., Petryniak, M. A., Shevchenko, E., McKinsey, G. L., Ekker, M., & Rubenstein, J. L. (2009). Generation of Cre-transgenic mice using Dlx1/Dlx2 enhancers and their characterization in GABAergic interneurons. Molecular and Cellular Neuroscience, 40(2), 167-186.

Puskarjov, M., Kahle, K. T., Ruusuvuori, E., & Kaila, K. (2014). Pharmacotherapeutic targeting of cation-chloride cotransporters in neonatal seizures. Epilepsia, 55(6), 806-818.

Putcha, D., Brickhouse, M., O'Keefe, K., Sullivan, C., Rentz, D., Marshall, G., ... & Sperling, R. (2011). Hippocampal hyperactivation associated with cortical thinning in Alzheimer's disease signature regions in non-demented elderly adults. Journal of Neuroscience, 31(48), 17680-17688.

Raber, J., Bongers, G., LeFevour, A., Buttini, M., & Mucke, L. (2002). Androgens protect against apolipoprotein E4-induced cognitive deficits. Journal of Neuroscience, 22(12), 5204-5209.

Raber, J., Huang, Y., & Ashford, J. W. (2004). ApoE genotype accounts for the vast majority of AD risk and AD pathology. Neurobiology of aging, 25(5), 641-650.

Rabinowicz, A. L., Starkstein, S. E., Leiguarda, R. C., & Coleman, A. E. (2000). Transient epileptic amnesia in dementia: a treatable unrecognized cause of episodic amnestic wandering. Alzheimer Disease & Associated Disorders, 14(4), 231-233.

Rolls, E. T. (1989). Functions of neuronal networks in the hippocampus and neocortex in memory. Academic Press.

Rolls, E. T. (2007). An attractor network in the hippocampus: theory and neurophysiology. Learning & Memory, 14(11), 714-731.

Romanova, T. V., & Rudzit, É. A. (1985). Comparative study of the diuretic action of bumetanide and other antidiuretic agents in mice. Pharmaceutical Chemistry Journal, 19(10), 706-708.

Semyanov, A., Walker, M. C., Kullmann, D. M., & Silver, R. A. (2004). Tonically active GABA A receptors: modulating gain and maintaining the tone. Trends in neurosciences, 27(5), 262-269.

Sen, A., Martinian, L., Nikolic, M., Walker, M. C., Thom, M., & Sisodiya, S. M. (2007). Increased NKCC1 expression in refractory human epilepsy. Epilepsy research, 74(2), 220-227.

Seymour, V. A., Curmi, J. P., Howitt, S. M., Casarotto, M. G., Laver, D. R., & Tierney, M. L. (2012). Selective modulation of different GABA A receptor isoforms by diazepam and etomidate in

hippocampal neurons. The international journal of biochemistry & cell biology, 44(9), 1491-1500.

Shimizu-Okabe, C., Okabe, A., Kilb, W., Sato, K., Luhmann, H. J., & Fukuda, A. (2007). Changes in the expression of cation-Cl− cotransporters, NKCC1 and KCC2, during cortical malformation induced by neonatal freeze-lesion. Neuroscience research, 59(3), 288-295.

Shu, H. J., Bracamontes, J., Taylor, A., Wu, K., Eaton, M. M., Akk, G., ... & Zorumski, C. F. (2012). Characteristics of concatemeric GABAA receptors containing α4/δ subunits expressed in Xenopus oocytes. British journal of pharmacology, 165(7), 2228-2243.

Sieghart, W., & Sperk, G. (2002). Subunit composition, distribution and function of GABA-A receptor subtypes. Current topics in medicinal chemistry, 2(8), 795-816.

Sivakumaran, S., & Maguire, J. (2016). Bumetanide reduces seizure progression and the development of pharmacoresistant status epilepticus. Epilepsia, 57(2), 222-232.

Smith, S. S., Shen, H., Gong, Q. H., & Zhou, X. (2007). Neurosteroid regulation of GABA A receptors: focus on the α4 and δ subunits. Pharmacology & therapeutics, 116(1), 58-76.

Song, I., Savtchenko, L., & Semyanov, A. (2011). Tonic excitation or inhibition is set by GABAA conductance in hippocampal interneurons. Nature communications, 2, 376.

Spigelman, I., Li, Z., Liang, J., Cagetti, E., Samzadeh, S., Mihalek, R. M., ... & Olsen, R. W. (2003). Reduced inhibition and sensitivity to neurosteroids in hippocampus of mice lacking the GABAA receptor δ subunit. Journal of neurophysiology, 90(2), 903-910.

Suvitayavat, W., Palfrey, H. C., Haas, M., Dunham, P. B., Kalmar, F., & Rao, M. C. (1994). Characterization of the endogenous Na (+)-K (+)-2Cl-cotransporter in Xenopus oocytes. American Journal of Physiology-Cell Physiology, 266(1), C284-C292.

Tang, Y., Scott, D. A., Das, U., Edland, S. D., Radomski, K., Koo, E. H., & Roy, S. (2012). Early and Selective Impairments in Axonal Transport Kinetics of Synaptic Cargoes Induced by Soluble Amyloid β-Protein Oligomers. Traffic, 13(5), 681-693.

Tong, L. M., Djukic, B., Arnold, C., Gillespie, A. K., Yoon, S. Y., Wang, M. M., ... & Huang, Y. (2014). Inhibitory interneuron progenitor transplantation restores normal learning and memory in ApoE4 knock-in mice without or with Aβ accumulation. Journal of Neuroscience, 34(29), 9506-9515.

Tong, L. M., Yoon, S. Y., Andrews-Zwilling, Y., Yang, A., Lin, V., Lei, H., & Huang, Y. (2016). Enhancing GABA signaling during middle adulthood prevents age-dependent GABAergic interneuron decline and learning and memory deficits in ApoE4 mice. Journal of Neuroscience, 36(7), 2316-2322.

Töllner, K., Brandt, C., Töpfer, M., Brunhofer, G., Erker, T., Gabriel, M., ... & Löscher, W. (2014). A novel prodrug-based strategy to increase effects of bumetanide in epilepsy. Annals of neurology, 75(4), 550-562.

Tornberg, J., Voikar, V., Savilahti, H., Rauvala, H., & Airaksinen, M. S. (2005). Behavioural phenotypes of hypomorphic KCC2-deficient mice. European Journal of Neuroscience, 21(5), 1327-1337.

Verghese, P. B., Castellano, J. M., & Holtzman, D. M. (2011). Apolipoprotein E in Alzheimer's disease and other neurological disorders. The Lancet Neurology, 10(3), 241-252.

Verret, L., Mann, E. O., Hang, G. B., Barth, A. M., Cobos, I., Ho, K., ... & Mucke, L. (2012). Inhibitory interneuron deficit links altered network activity and cognitive dysfunction in Alzheimer model. Cell, 149(3), 708-721.

Vorhees, C. V., & Williams, M. T. (2006). Morris water maze: procedures for assessing spatial and related forms of learning and memory. Nature protocols, 1(2), 848-858.

Wafford, K. A., Van Niel, M. B., Ma, Q. P., Horridge, E., Herd, M. B., Peden, D. R., ... & Lambert, J. J. (2009). Novel compounds selectively enhance δ subunit containing GABA A receptors and increase tonic currents in thalamus. Neuropharmacology, 56(1), 182-189.

Walf, A. A., & Frye, C. A. (2007). The use of the elevated plus maze as an assay of anxiety-related behavior in rodents. Nature protocols, 2(2), 322-328.

Walker MC & Kullmann DM (2012) Tonic GABAA receptor-mediated signaling in epilepsy. From Jasper's Basic Mechanisms of the Epilepsies 80 (2012): 111.

Wang, D. D., & Kriegstein, A. R. (2011). Blocking early GABA depolarization with bumetanide results in permanent alterations in cortical circuits and sensorimotor gating deficits. Cerebral Cortex, 21(3), 574-587.

Wei, W., Zhang, N., Peng, Z., Houser, C. R., & Mody, I. (2003). Perisynaptic localization of δ subunit-containing GABAA receptors and their activation by GABA spillover in the mouse dentate gyrus. Journal of Neuroscience, 23(33), 10650-10661.

Whissell, P. D., Rosenzweig, S., Lecker, I., Wang, D. S., Wojtowicz, J. M., & Orser, B. A. (2013). γ-aminobutyric acid type A receptors that contain the δ subunit promote memory and neurogenesis in the dentate gyrus. Annals of neurology, 74(4), 611-621.

Whiting, P. J. (2003). GABA-A receptor subtypes in the brain: a paradigm for CNS drug discovery? Drug discovery today, 8(10), 445-450.

Wisden, W., Laurie, D. J., Monyer, H., & Seeburg, P. H. (1992). The distribution of 13 GABAA receptor subunit mRNAs in the rat brain. I. Telencephalon, diencephalon, mesencephalon. Journal of Neuroscience, 12(3), 1040-1062.

Wu, L., & Zhao, L. (2016). ApoE2 and Alzheimer's disease: time to take a closer look. Neural regeneration research, 11(3), 412.

Yang, S., Cohen, C. J., Peng, P. D., Zhao, Y., Cassard, L., Yu, Z., ... & Morgan, R. A. (2008). Development of optimal bicistronic lentiviral vectors facilitates high-level TCR gene expression and robust tumor cell recognition. Gene therapy, 15(21), 1411-1423.

Ye, Z. Y., Li, D. P., Byun, H. S., Li, L., & Pan, H. L. (2012). NKCC1 upregulation disrupts chloride homeostasis in the hypothalamus and increases neuronal activity–sympathetic drive in hypertension. Journal of Neuroscience, 32(25), 8560-8568.

Yeckel, M. F., & Berger, T. W. (1990). Feedforward excitation of the hippocampus by afferents from the entorhinal cortex: redefinition of the role of the trisynaptic pathway. Proceedings of the National Academy of Sciences, 87(15), 5832-5836.

Yeo, M., Berglund, K., Augustine, G., & Liedtke, W. (2009). Novel repression of Kcc2 transcription by REST–RE-1 controls developmental switch in neuronal chloride. Journal of Neuroscience, 29(46), 14652-14662.

Zhou, C., Huang, Z., Ding, L., Deel, M. E., Arain, F. M., Murray, C. R., ... & Gallagher, M. J. (2013). Altered cortical GABAA receptor composition, physiology, and endocytosis in a mouse model of a human genetic absence epilepsy syndrome. Journal of Biological Chemistry, 288(29), 21458-21472.

Zimmer, R., Teelken, A. W., Trieling, W. B., Weber, W., Weihmayr, T., & Lauter, H. (1984). γ-Aminobutyric acid and homovanillic acid concentration in the CSF of patients with senile dementia of Alzheimer's type. Archives of neurology, 41(6), 602-604.

PUBLISHING AGREEMENT

It is the policy of the University to encourage the distribution of all theses, dissertations, and manuscripts. Copies of all UCSF theses, dissertations, and manuscripts will be routed to the library via the Graduate Division. The library will make all theses, dissertations, and manuscripts accessible to the public and will preserve these to the best of their abilities, in perpetuity.

I hereby grant permission to the Graduate Division of the University of California, San Francisco to release copies of my thesis, dissertation, or manuscript to the Campus Library to provide access and preservation, in whole or in part, in perpetuity.

Author Signature 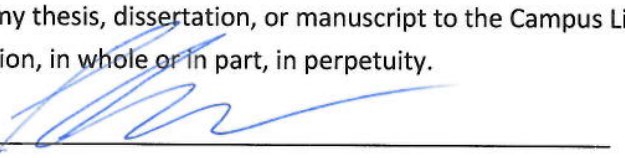

Date 8/5/2017